DEVELOPMENT OF NATURAL RUBBER COMPOSITE FOR CEMENTITIOUS MATERIALS

NAMTHIP BUREEWONG

A Thesis Submitted in Partial Fulfillment of the Requirements for the
Degree of Master of Engineering in Materials Engineering
Suranaree University of Technology
Academic Year 2022

การพัฒนายางธรรมชาติคอมโพสิทสำหรับการใช้ในวัสดุซีเมนต์

นางสาวน้ำทิพย์ บุรีวงค์

วิทยานิพนธ์นี้เป็นส่วนหนึ่งของการศึกษาตามหลักสูตรปริญญาวิศวกรรมศาสตรมหาบัณฑิต
สาขาวิชาวิศวกรรมวัสดุ
มหาวิทยาลัยเทคโนโลยีสุรนารี
ปีการศึกษา 2565

DEVELOPMENT OF NATURAL RUBBER COMPOSITE FOR CEMENTITIOUS MATERIALS

Suranaree University of Technology has approved this thesis submitted in partial fulfillment of the requirements for a Master's Degree.

Thesis Examining Committee

.....

(Assoc. Prof. Dr.Wimonlak Sutapun)
Chairperson

.....

(Assoc. Prof. Dr.Chaiwat Ruksakulpiwat)
Member (Thesis Advisor)

.....

(Assoc. Prof. Dr.Yupaporn Ruksakulpiwat)
Member (Thesis Co-advisor)

.....

(Assoc. Prof. Dr.Sittipong Amnuaypanich)
Member

.....

(Asst. Prof. Dr.Nitinat Suppakarn)
Member

.....

(Assoc. Prof. Dr.Chatchai Jothityangkoon)
Vice Rector for Academic
Affairs and Quality Assurance

.....

(Assoc. Prof. Dr.Pornsiri Jongkol)
Dean of Institute of Engineering

น้ำทิพย์ บุรีวงค์: การพัฒนายางธรรมชาติคอมโพสิทสำหรับการใช้ในวัสดุซีเมนต์ (DEVELOPMENT OF NATURAL RUBBER COMPOSITE FOR CEMENTITIOUS MATERIALS) อาจารย์ที่ปรึกษา: รองศาสตราจารย์ ดร. ไชยวัฒน์ รักสกลุพิวัฒน์, 84 หน้า

คำสำคัญ: ยางธรรมชาติ/ยางคาร์บอกซีเลเต็ดสไตรีนบิวทาไดอีน/ไวนิลไตรเอทอกซีไซเลน/ซิลิกา/เถ้าแกลบข้าว/ยางคอมโพสิท/มอร์ต้าดัดแปลงด้วยพอลิเมอร์

ในวิทยานิพนธ์นี้มีวัตถุประสงค์เพื่อพัฒนายางธรรมชาติเป็นน้ำยางพอลิเมอร์ที่ใช้ดัดแปลงมอร์ต้าเพื่อความยั่งยืนและมีประสิทธิภาพ โดยยางธรรมชาติที่ใช้จะมีการเติมซิลิกาที่เตรียมได้จากเถ้าแกลบข้าวโดยใช้วิธีการตกตะกอนร่วมด้วย

ซิลิกาที่เตรียมได้จากเถ้าแกลบข้าวโดยใช้วิธีการตกตะกอนมีความบริสุทธิ์สูงถึงร้อยละ 99 และมีโครงสร้างในรูปแบบอสัญฐาน นอกจากนี้เมื่อเปรียบเทียบซิลิกาที่เตรียมได้กับซิลิกาทางการค้า พบว่า ซิลิกาที่เตรียมได้มีขนาดของอนุภาคที่เล็กกว่าและมีพื้นที่ผิวที่สูงกว่าซิลิกาทางการค้า

การเติมซิลิกาที่เตรียมได้ลงในยางธรรมชาติที่ปริมาณการเติม 0, 5, 10, และ 20 ส่วนในร้อยส่วนของยางพบว่า ค่าทอร์กต่ำสุดของยางธรรมชาติคอมโพสิทเพิ่มขึ้นตามปริมาณของซิลิกาที่เพิ่มขึ้น แต่เวลาสกอร์ชและเวลาคงรูปของยางธรรมชาติลดลงเมื่อเติมซิลิกา ค่าโมดูลัสที่ร้อยละ 100 และ 300 ของการยืดของยางธรรมชาติคอมโพสิทเพิ่มขึ้นอย่างไม่มีนัยสำคัญตามปริมาณของซิลิกาที่เพิ่มขึ้น เช่นเดียวกับค่าความแข็ง ค่าความต้านทานต่อแรงดึงของยางธรรมชาติคอมโพสิทเพิ่มขึ้นตามปริมาณของซิลิกาที่เพิ่มขึ้นเช่นเดียวกับค่าร้อยละของการยืดก่อนขาดที่มีแนวโน้มเพิ่มขึ้น การใช้ไวนิลไตรเอทอกซีไซเลนร่วมกับซิลิกา และเติมลงในยางธรรมชาติที่ปริมาณการเติมต่างๆ โดยกำหนดอัตราส่วนระหว่างไวนิลไตรเอทอกซีไซเลนกับซิลิกาที่ 1 ต่อ 10 พบว่า ค่าทอร์กต่ำสุดและค่าทอร์กสูงสุดของยางธรรมชาติเพิ่มขึ้น แต่ค่าเวลาสกอร์ชและเวลาคงรูปของยางธรรมชาติลดลงเมื่อเติมซิลิกา ค่าโมดูลัสที่ร้อยละ 100 และ 300 ของการยืดของยางธรรมชาติเพิ่มขึ้นเมื่อเติมซิลิกา โดยที่ปริมาณการเติมของซิลิกา 5 และ 10 ส่วนในร้อยส่วนของยางแสดงค่าของคุณสมบัติเหล่านี้ที่ใกล้เคียงกันเช่นเดียวกับค่าความต้านทานต่อแรงดึงและค่าร้อยละของการยืดก่อนขาด ค่าความแข็งของยางธรรมชาติคอมโพสิทเพิ่มขึ้นตามปริมาณของซิลิกาที่เพิ่มขึ้น การผสมยางธรรมชาติกับยางคาร์บอกซีเลเต็ดสไตรีนบิวทาไดอีนที่อัตราส่วน 2 ต่อ 1 และเติมซิลิกาที่ปริมาณต่างๆ พบว่า การเพิ่มขึ้นของปริมาณซิลิกาในยางผสมทำให้เวลาสกอร์ชและเวลาคงรูปของยางคอมโพสิทลดลง แต่ค่าโมดูลัสที่ร้อยละ 100 และ 300 ของการยืดของยางคอมโพสิทเพิ่มขึ้นเช่นเดียวกับค่าความแข็ง สำหรับค่าทอร์กสูงสุด ค่าความต้านทานต่อ

แรงดึงและค่าร้อยละของการยืดก่อนขาดของยางคอมโพสิทแสดงค่าสูงสุดที่ปริมาณการเติมของซิลิกา 5 ส่วนในร้อยส่วนของยาง การเติมซิลิกาลงในยางผสมแสดงค่าความต้านทานต่อแรงดึงและค่าร้อยละของการยืดก่อนขาดสูงกว่าการเติมซิลิการ่วมกับไวนิลไตรเอทอกซีไซเลนลงในยางธรรมชาติ ดังนั้น การเติมซิลิกาลงในยางผสมที่ปริมาณการเติม 5 ส่วนในร้อยส่วนของยางนี้ จะถูกใช้เป็นพอลิเมอร์สำหรับการศึกษาถัดไป

การเติมพอลิเมอร์ลงในซีเมนต์ที่อัตราส่วนระหว่างพอลิเมอร์ต่อซีเมนต์ 0.00, 0.05, 0.10, และ 0.20 พบว่า เมื่อเปรียบเทียบมอร์ต้าดัดแปลงด้วยพอลิเมอร์ที่ปริมาณการเติม 0.05, 0.10, และ 0.20 มอร์ต้าดัดแปลงด้วยพอลิเมอร์ที่ปริมาณการเติม 0.10 แสดงค่าความต้านทานต่อแรงดึง ค่าความต้านทานต่อแรงดัดโค้งและค่าความต้านทานต่อแรงกดอัดสูงสุด นอกจากนี้ยังลดค่าการดูดซึมน้ำได้สูงสุดอีกด้วย

สาขาวิชา วิศวกรรมพอลิเมอร์ ลายมือชื่อนักศึกษา .....

ปีการศึกษา 2565 ลายมือชื่ออาจารย์ที่ปรึกษา .....

ลายมือชื่ออาจารย์ที่ปรึกษาร่วม .....

NAMTHIP BUREEWONG: DEVELOPMENT OF NATURAL RUBBER COMPOSITE FOR CEMENTITIOUS MATERIALS. THESIS ADVISOR: ASSOC. PROF. CHAIWAT RUKSAKULPIWAT, Ph.D., 84 PP.

Keyword: NATURAL RUBBER/CARBOXYLATED STYRENE BUTADIENE RUBBER/VINYL-TRIETHOXYSILANE/SILICA/RICE HUSK ASH/RUBBER COMPOSITE/POLYMER-MODIFIED MORTAR

In this research, the aim is to develop natural rubber (NR) as a polymer latex combined with silica extracted from rice husk ash (RHA) by the precipitation method for producing polymer-modified mortar (PMM) that is effective and sustainable.

Rice husk silica (RSi) had a purity of up to 99% and had a typical amorphous form. When comparing the RSi with commercial silica (CSi), it was found that RSi had a smaller particle size and a higher surface area than CSi.

The addition of RSi to NR at the contents of 0, 5, 10, and 20 phr showed that the minimum torque (ML) of NR increased with increasing RSi content. However, the scorch time (ts2) and optimal cure time (tc90) of NR decreased when RSi was added. The modulus at 100% elongation (M100), modulus at 300% elongation (M300), and hardness of composite increased insignificantly with increasing RSi content. Nevertheless, the tensile strength and elongation at break of NR increased with increasing RSi content. Vinyltriethoxysilane (VTES) mixed with RSi in a ratio of 1:10 was added to NR at different RSi contents. It was found that with the addition of VTES/RSi, the ML and maximum torque (MH) of NR increased but the ts2 and tc90 of NR decreased. The M100, M300, tensile strength, and elongation at break of NR increased with the addition of RSi up to 5 phr. The hardness of NR increased with increasing RSi content. NR was mixed with carboxylated styrene butadiene rubber (XSBR) at a ratio of 2:1 and adding RSi at different contents form 0 to 20 phr. With the increase in RSi content, the ts2 and tc90 of composite decreased but the M100, M300, and hardness of composite increased. The highest values of MH, tensile strength, and elongation at

break were obtained with the addition of RSi at 5 phr. The addition of RSi to the blend showed higher tensile strength and elongation at break than adding VTES/RSi to NR. So, the optimum content of RSi of 5 phr was used.

The polymer was added to cement at the polymer to cement (P/C) ratios of 0.00, 0.05, 0.10, and 0.20. The addition of polymer to cement up to P/C ratio of 0.10 led to an increase in tensile strength, flexural strength, and compressive strength. Also, the highest reduction of water absorption was achieved.

School of Polymer Engineering

Academic Year 2022

Student's Signature Namthip Bureewong

Advisor's Signature .....

Co-advisor's Signature .....

ACKNOWLEDGEMENT

I gratefully acknowledge the Center of Excellence on Petrochemical and Materials Technology and the Research Center for Biocomposite Materials for Medical Industry and Agricultural and Food Industry for their financial support.

First, I am deeply grateful and appreciative to my thesis advisor, Assoc. Prof. Dr. Chaiwat Ruksakulpiwat, for his invaluable suggestions, inspiring guidance, and supporting information throughout the period of study. I also want to thank my thesis advisor for his tireless effort in encouraging me to complete my work. Sincere appreciation is also extended to the thesis co-advisor, Assoc. Prof. Dr. Yupaporn Ruksakulpiwat, for her invaluable suggestions during my research work. In addition, I gratefully thank the chairperson, Assoc. Prof. Dr. Wimonlak Sutapun, and the committee, Assoc. Prof. Dr. Sittipong Amnuaypanich, Asst. Prof. Dr. Nitinat Suppakarn, and Assoc. Prof. Dr. Yupaporn Ruksakulpiwat, for their invaluable suggestions and encouragement.

My appreciation also goes to all staff members and all friends of the School of Polymer Engineering for their help and support throughout my work.

Finally, my graduation would not be achieved without the best wishes of my parents, who have given me an invaluable life with their unconditional love, encouragement, and support throughout my life.

Namthip Bureewong

TABLE OF CONTENTS

Page

TABLE OF CONTENTS (Continued)

Page

TABLE OF CONTENTS (Continued)

Page

LIST OF TABLES

Table **Page**

LIST OF FIGURES

Figure **Page**

LIST OF FIGURES (Continued)

Figure **Page**

SYMBOLS AND ABBREVIATIONS

%	=	Percent
MPa	=	Mega Pascal
g	=	Gram
N	=	Normality
pH	=	Potential of hydrogen ion
^{o}C	=	Degree Celsius
nm	=	Nanometer
m^2/g	=	Square meter per gram
M	=	Molarity
rpm	=	Revolutions per minute
wt%	=	Weight percentage
mm	=	Millimeter
cm^{-1}	=	Reciprocal centimeter
θ	=	Theta
kN	=	Kilonewton
mm/min	=	Millimeter per minute
kN/s	=	Kilonewton per second
N	=	Newton
mm^2	=	Square millimeter
g/cm^2	=	Gram per square centimeter
cm^3/g	=	Cubic centimeter per gram
dNm	=	Decinewton meter
SiO_2	=	Silicon dioxide
K_2O	=	Potassium oxide
CaO	=	Calcium oxide
TiO_2	=	Titanium dioxide

SYMBOLS AND ABBREVIATIONS (Continued)

MnO_2	=	Manganese dioxide
Fe_2O_3	=	Iron(III) oxide
C	=	Carbon
O	=	Oxygen
Mg	=	Magnesium
Al	=	Aluminum
Si	=	Silicon
Ca	=	Calcium

CHAPTER 1
INTRODUCTION

1.1 General background

Polymer-modified mortar (PMM) is an ordinary mortar with added polymer in latex form that are used in applications such as paving and waterproofing materials, floorings, grouting wall and floor tile, patch and repair, and anticorrosive linings. This is because the use of polymer latex in mortar usually improves the tensile and flexural strengths, adhesion, extensibility, and durability of the ordinary mortar by waterproofness and chemical resistance (Ohama & Ramachandran, 1996). In the present, the polymer types that are used in mortar can be divided into two types as synthetic and natural polymers. Examples of synthetic polymers such as polyacrylate (PAE), styrene butyl acrylate (SBA), ethylene vinyl acetate (EVA), carboxylated styrene butadiene rubber (XSBR), styrene butadiene rubber (SBR), chloroprene rubber (CR), polyvinyl alcohol (PVA), etc. For the natural polymer as natural rubber (NR) (Ohama & Ramachandran, 1996; Zhang et al., 2021). However, the compressive strength of most PMM is lower than ordinary mortar. To resolve this issue, the use of silica combined with polymer in mortar is an alternative way. This is because the use of silica in mortar usually improves the compressive strength of ordinary mortar by having a pore-filling effect (Aggarwal et al., 2015).

Currently, several industries, including the construction industry are focused on using local and natural materials from renewable resources to produce products with the required properties. Thus, the development of PMM to be more effective and sustainable with the use of materials from natural sources is an interesting approach. For example, the use of natural rubber latex (NRL) combined with silica extracted from natural sources. NR is a natural polymer that is obtained from the *Hevea brasiliensis* tree or Para rubber tree in latex form and consists mainly of two components are small particles of rubber and water. Additionally, some minor components such as proteins,

lipids, carbohydrates, and inorganic components. In the present, NR in latex and solid forms is used as raw material to produce the many products that cover several industries such as automotive, medical, and others. Examples of NR products include tires, belts, seals, gloves, tubes, etc. (Rajan et al., 2006). This is because it has high resilience, good tensile strength, good tear resistance, etc. (Chuayjuljit et al., 2015; Vu et al., 2015). For the silica is currently extracted from several natural sources such as corn cob, sugarcane bagasse ash, bamboo, rice straw, rice husk ash, and others. The preparation of silica using rice husk ash (RHA) is an interesting approach because normally it contains a high silica content of over 60%. Furthermore, RHA is the by-product of the process of rice husk (RH) pyrolysis for energy production, which is usually dumped in landfills, leading to air and water pollution. To reduce this issue and increase the value of this material, the current use of RHA is in many applications such as fertilizer, adsorbent and catalyst in the form of activated carbon or silica, and in the cement and concrete industries in the form of silicate or silica, etc. (Pode, 2016; Shen, 2017; Shen et al., 2014). However, it is known that NR and silica are generally incompatible due to the non-polarity and polarity of materials. Thus, to improve the functionality of materials, requiring the use of vinyltriethoxysilane (VTES) as a compatibilizer or XSBR combined in the system may reduce this issue.

In this research, the aim is to develop NR as a polymer latex combined with silica extracted from RHA by the precipitation method for producing PMM that is effective and sustainable. The rice husk silica (RSi) was compared with commercial silica (CSi) before being used as a filler in the rubber matrix. Additionally, VTES or XSBR in latex form was used to improve the functionality between NR and RSi.

1.2 Research objectives

The main objectives of this research work are as follows:

1.2.1 To study the chemical and physical properties of prepared RSi compared with CSi.

1.2.2 To study the effects of RSi content on cure characteristics, mechanical properties, and morphological properties of rubber composites.

1.2.3 To study the effects of polymer content on mechanical, durability, and morphological properties of PMM.

1.3 Scope and limitation of the study

The RSi that was prepared from RHA by the precipitation method is compared with CSi in terms of chemical and physical properties by using the Fourier transform infrared spectrometer (FTIR), energy dispersive X-ray fluorescence spectrometer (EDXRF), X-ray diffractometer (XRD), Branauer-Emmett-Teller (BET) analysis, dynamic light scattering (DLS) measurement, and field emission scanning electron microscope (FESEM).

The addition of RSi at the contents of 0, 5, 10, and 20 phr in NR was studied on cure characteristics, mechanical properties, and morphological properties by using the moving die rheometer (MDR), universal testing machine (UTM), hardness tester, and FESEM. The comparison of using VTES and XSBR in combination with NR and RSi with the RSi contents at 0, 5, 10, and 20 phr were also studied on cure characteristics, mechanical properties, and morphological properties. For NR/VTES/RSi composites, the use of VTES with RSi was fixed at a ratio of 1:10. For NR/XSBR/RSi composites, the blending of XSBR in NR was fixed at a ratio of 2:1. All the rubber composites were first prepared by wet-mixing and drying to obtain the rubber composite sheets. Then the previous rubber composite sheets were compounded with chemicals using a two-roll mill and vulcanized using a compression molding machine.

Based on the mechanical properties of all rubber composites, the rubber composite with the optimal mechanical properties was selected to be used as a polymer in further study. The polymer was added to cement at the polymer to cement (P/C) ratios of 0.00, 0.05, 0.10, and 0.20 to obtain PMM. All the samples were mixed according to ASTM C305 and cured in water for 28 days before testing. The mechanical, durability, and morphological properties were studied.

CHAPTER 2

LITERATURE REVIEWS

2.1 Polymer-modified mortar

Normally, polymer-modified mortar (PMM) is an ordinary mortar with added polymer in latex form, which the mix proportions of PMM are in the mass ratios of polymer to cement (P/C) in the range of 0.05 to 0.20, the cement to sand (C/S) in the range of 0.30-0.50, and the water to cement (W/C) in the range of 0.30-0.60 that depend on the required properties. In the present, PMM are used in applications such as paving and waterproofing materials, floorings, grouting wall and floor tile, patch and repair, and anticorrosive linings because the use of polymer latex in mortar usually improves the tensile and flexural strengths, adhesion, extensibility, and durability of the ordinary mortar by waterproofness and chemical resistance (Ohama & Ramachandran, 1996). For the improved flexural strength of PMM, Wang et al. (2016) give the physical model of PMM when the force in flexural mode is applied, as shown in Figure 2.1.

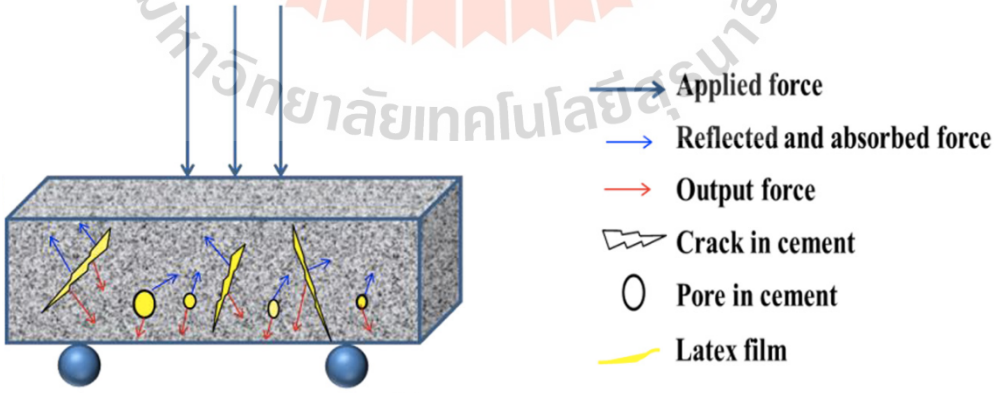

Figure 2.1 Physical model of PMM when the force in flexural mode is applied (Wang et al., 2016).

Figure 2.1 represents the polymer latex films and particles that absorb and reflect a part of the applied force during the flexural mode, improving the flexural strength of PMM. The polymer types that are used in mortar can be divided into two types as synthetic and natural polymers. Examples of synthetic polymers such as polyacrylate (PAE), styrene butyl acrylate (SBA), ethylene vinyl acetate (EVA), carboxylated styrene butadiene rubber (XSBR), styrene butadiene rubber (SBR), chloroprene rubber (CR), polyvinyl alcohol (PVA), etc. For the natural polymer as natural rubber (NR) (Ohama & Ramachandran, 1996; Zhang et al., 2021). The procedures for preparing the PMM currently have three methods, as shown in Figure 2.2. Figure 2.2a represents the mixture of water, admixture, and polymer latex directly added to the pre-mixed powders of cement and sand. Figure 2.2b represents the polymer latex added to the prepared fresh mortar. Figure 2.2c represents the preparation of water mixed with polymer latex and water mixed with mortar separately, then mixing these two mixtures together. However, there is no universal method for preparing the PMM. For a good mix, the method should be suitable for the type of polymer used in mortar (Zhang et al., 2021). The quality requirements for the PMM in JIS A 6203 are listed in Table 2.1.

Table 2.1 Quality requirements of PMM in JIS A 6203.

Properties	Requirement
Flexural strength	Not less than 3.9 MPa
Compressive strength	Not less than 9.8 MPa
Adhesion	Not less than 0.98 MPa
Water absorption	Not more than 15%
Amount of water permeation	Not more than 30 g
Length change	0 to 0.15%

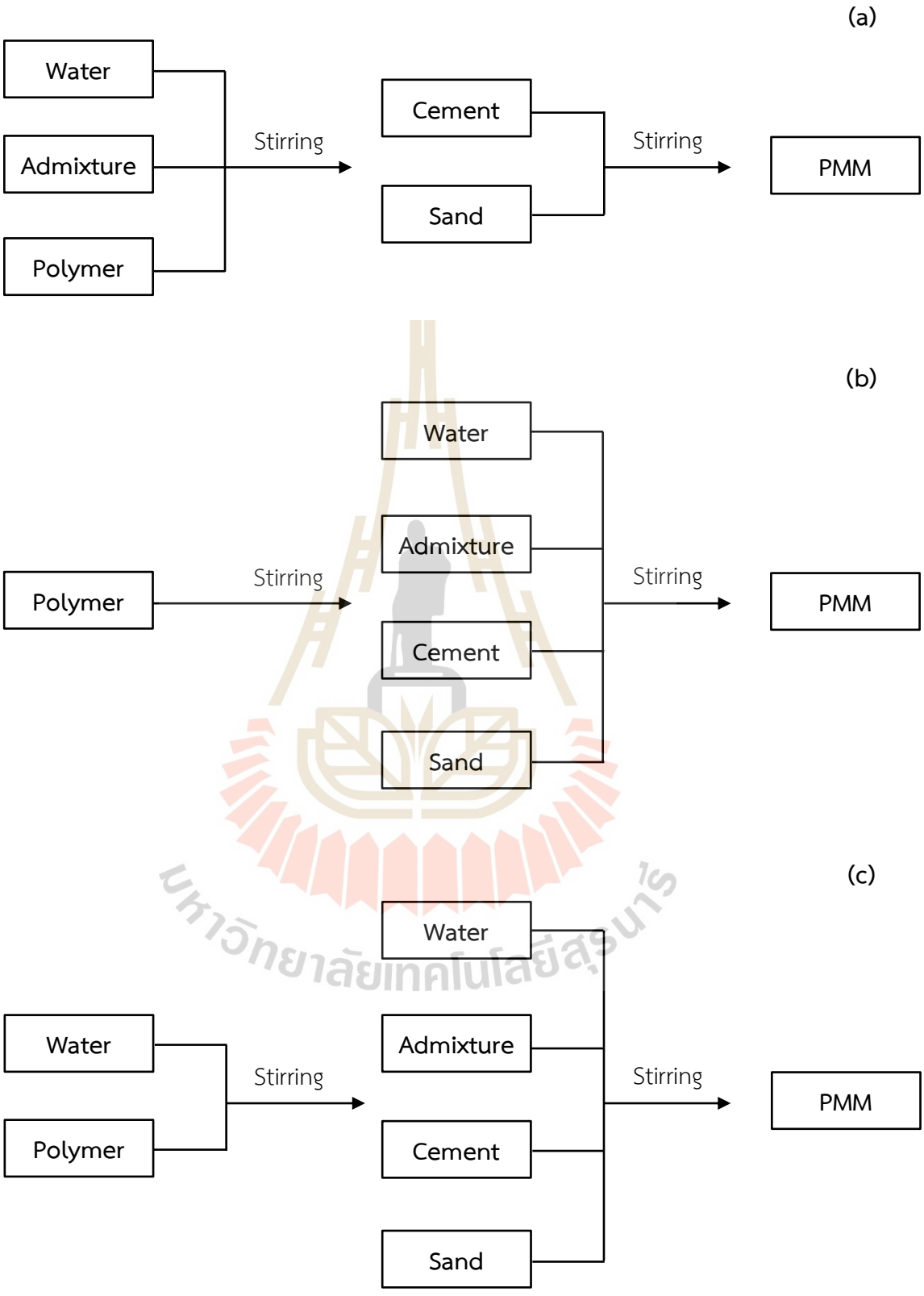

Figure 2.2 Schematic diagram of PMM preparation procedures.

2.2 Effect of the addition of polymer latex in mortar

2.2.1 Synthetic polymer

Knapen & Van Gemert (2015) reported the effects of addition of PVA in mortar at a P/C ratio of 0.01 on the compressive and flexural properties. For the mortar that cures in the water for 28 days, the result shows that the addition of PVA decreased the compressive strength of ordinary mortar because of air entrainment. However, the flexural strength of mortar added with PVA increased by more than 21% of the flexural strength value of ordinary mortar. This is because of the formation of PVA films in mortar.

Assaad (2018) reported the effects of additions of SBR and PVA in mortar at different contents on the compressive and flexural properties. When considered only the mortar that mixes by post-addition, fixes the ratio of W/C at 0.50, and cures for 28 days. The addition of SBR and PVA decreased the compressive strength of ordinary mortar. Because the addition of polymer in mortar retarded cement hydration, which increased porosity and weakened the mortar structure. While the flexural strength of mortar added with SBR and PVA increased with increasing the P/C ratio. This is because the polymer films can bridge the microcracks and reduce their propagation during the tensile loading. Moreover, considering the effects of different polymer types that were added in mortar at the same content on these properties, the result shows that all mortar with added SBR had a higher value than mortar with added PVA.

Wang et al. (2015) reported the effect of additions of SBR and styrene acrylic ester (SAE) in mortar at the P/C ratios of 0.01, 0.03, 0.05, 0.08, 0.10, 0.12, 0.15, 0.18, and 0.20 on the durability property in term of waterproofness. For the mortar that cures for 28 days, the water absorption resistance of mortar added with SBR and SAE increased with increasing the P/C ratio. For mortar added with SBR, the influence of increasing the P/C ratio on water absorption is not significant when the P/C ratio is more than 0.08. As the mortar is added with SAE, the influence of increasing the P/C ratio on water absorption is not significant when the P/C ratio is more than 0.10. Thus, the optimal conditions on this property are the addition of SBR and SAE in mortar at the P/C ratios of 0.08 and 0.10, respectively.

Baghini et al. (2016) reported the effects of addition of XSBR in mortar at the XSBR contents of 0.05, 0.06, 0.07, 0.08, 0.09, and 0.10 on the mechanical properties. For the mortar that cures for 28 days, the unconfined compressive strength and abrasion resistance of mortar added with XSBR increased with increasing XSBR contents until it reached a XSBR content of 0.08. This is because both flexible butadiene chains and rigid styrene chains in the XSBR molecular structure provide good mechanical properties. However, the increment of XSBR content in mortar more than this content decreased these properties because the excess water from XSBR inhibited adequate mortar compaction.

2.2.2 Natural polymer

In the present, the natural polymer latex that is used in mortar has the only one as a natural rubber (NR). NR is a natural polymer that is obtained from the *Hevea brasiliensis* tree or Para rubber tree in latex form and consists mainly of two components are small particles of rubber and water. Additionally, some minor components such as proteins, lipids, carbohydrates, and inorganic components. Generally, the rubber particles in natural rubber latex (NRL) have spherical particles, which consist of 20 to 45% of the latex volume and are stabilized by the negative charge of surface surrounded by a mixed-layer of absorbed proteins and phospholipids. Currently, the possible model for NR particles has two models, as shown in Figure 2.3.

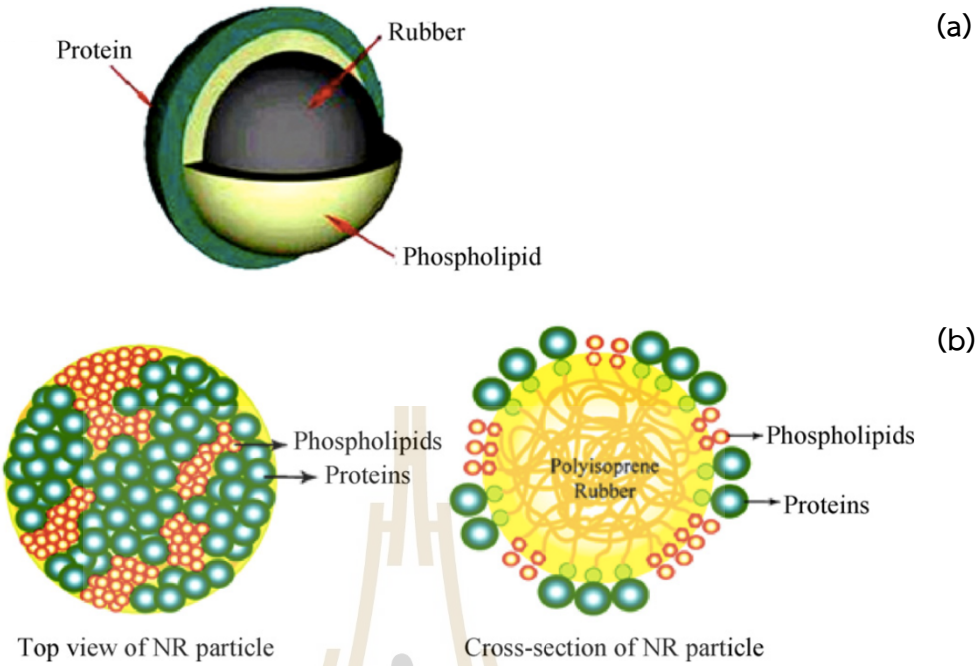

Figure 2.3 NR particle models (Wei et al., 2017).

Figure 2.3a represents the NR particle surrounded by a double-layer of proteins and phospholipids and Figure 2.3b represents the NR particle surrounded by a mixed-layer of proteins and phospholipids (Nawamawat et al., 2011; Vo & Plank, 2018; Wei et al., 2017). The most chemical structure of NR is cis-1,4-polyisoprene, as shown in Figure 2.4.

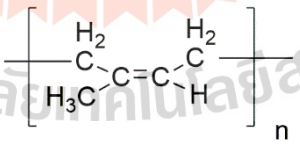

Figure 2.4 Chemical structure of cis-1,4-polyisoprene.

Currently, NR in latex and solid forms is used as raw material to produce the many products that cover several industries such as automotive, medical, and others. Examples of NR products include tires, belts, seals, gloves, tubes, etc. (Rajan et al., 2006). This is because it has high resilience, good tensile strength, good tear resistance, etc. (Chuayjuljit et al., 2015; Vu et al., 2015). However, to obtain the product properties as required, many NR products usually combine with other rubber, filler, or

both. Several times, there is an issue with incompatibility between NR and combinations, requiring the use of additives in the system to improve the functionality of materials. The common fillers that are used in the rubber industry include carbon black, silica, calcium carbonate, clay, fiber, etc. (Abdul Salim et al., 2018; Wongsorat et al., 2014). In addition, the use of NR, especially in latex form is also found in the construction industry in its applications as a modifier in asphalt, concrete, and mortar.

Sukmak et al. (2020) studied the effects of addition content of NRL in paste at the P/C ratios of 0.10, 0.20, 0.30, 0.40, and 0.50 on the mechanical properties. All the pastes were fixed the ratios of W/C at 0.55 and SDS/P at 0.10, where the SDS is a sodium dodecyl sulfate that used to provide the stability of NR particles. Then it was cured at a controlled air temperature for 28 days before testing. The addition of NRL in paste was found to improve the flexural strength and toughness of ordinary paste. On the other hand, the compressive strength of paste with added NRL was found to decrease this property of ordinary paste. This is because of the retardation effect from the presence of NR films and air bubble pores. In this study, the addition content of NRL in paste at a P/C ratio of 0.10 is an optimal condition, which provides the highest compressive and flexural strengths of all the paste with added NRL.

Loykaew & Utara (2020) studied the effect of replacement content of cement by NRL at 3, 6, 9, and 12% by weight on the durability property of paste in the acid and sulfate environments. All the pastes were used with the SDS to improve the compatibility between NRL and cement. Then it was cured in water for 28 days before testing. Based on the result of compressive strength, the replacement content of cement by NRL at 12% by weight is optimal, which increases the stability of paste after acid and sulfate immersions. This is because the NR films can exhibit the diffusion of acid and sulfate that help join the cement components together. Moreover, when compared to the paste with replaced NRL at the same immersion time, the paste with replaced NRL showed greater resistance to sulfate than acid environments.

Yaowarat et al. (2021) studied the effects of addition of NRL in concrete at different contents on the compressive and flexural properties. Considering only the concrete, which fixes the ratio of W/C at 0.30 and cures for 28 days. The results show the compressive strength of concrete added with NRL decreased with increasing the

P/C ratio. This is because the NR formed the thick films around the cement, which retarded its hydration. While the flexural strength of concrete added with NRL increased with the highest value was found in the P/C ratio at 0.58% by weight because the films enhanced the cohesion among the aggregate particles that improve the flexural strength of ordinary concrete. Moreover, this study suggested that this condition met the minimum requirements for compressive and flexural strengths for concrete pavement specified by the Department of Highways, Thailand.

However, the use of synthetic and natural polymers in latex form results in the same trend that enhances the tensile and flexural strength, extensibility, adhesion, and durability of ordinary mortar through waterproofness and chemical resistance. On the other hand, the compressive strength of most PMM is lower than ordinary mortar. To resolve this issue, the use of silica combined with polymer in mortar is an alternative way. This is because the use of silica in mortar usually improves the compressive strength of ordinary mortar by having a pore-filling effect (Aggarwal et al., 2015).

2.3 Effect of the addition of silica in mortar

Rupasinghe et al. (2017) reported the effect of replacement content of cement by nano-silica at 4, 8, and 12% by weight on the compressive property. The replacement of cement with nano-silica increased the compressive strength of ordinary paste. In this research, the optimal replacement content of cement by nano-silica was found at 8% by weight. As the replacement content of cement by nano-silica exceeds 8% by weight, the overall hydrated phase volume and the capillary pore volume of paste decrease and increase, respectively, which reduce the compressive strength.

Khan et al. (2020) reported the effects of micro-silica extracted from rice husk ash and used to replace cement in mortar at the contents of 5, 15, and 25% by weight on the compressive and flexural properties. For the mortar that cures in the air for 28 days, the replacement of cement by micro-silica increased the compressive and flexural strengths of ordinary mortar. In this research, the highest values of compressive and flexural strength were found in the replacement content of cement by micro-silica

at 5% by weight. As the replacement of cement by micro-silica is more than this content, the micro-silica agglomerates and forms the weak point in mortar.

Jo et al. (2007) reported the effect of nano-silica and silica fume replacing cement in mortar at different contents on the compressive property. The result shows the compressive strength of all mortars replacing cement with nano-silica was higher than the mortars replacing cement with silica fume. Because the nano-silica is more effective in the pozzolanic reaction than the silica fume that fills the pores of ordinary mortar. In this research, the highest compressive strength was found in the replacement content of cement by nano-silica at 12% by weight with the value of 68.80 MPa after curing in water for 28 days.

According to the literature, the current silica used in mortar derives from both natural and synthetic extractions. In addition, the current silica used in mortar is found in nano- and micro-sized particles. When comparing the silica source and silica size, the literature reveals that the silica size is more important to mortar properties than the silica source. Currently, several industries, including the construction industry are focused on using local and natural materials from renewable resources to produce products with the required properties. Thus, the development of PMM to be more effective and sustainable with the use of materials from natural sources is an interesting approach. For example, the use of NRL combined with nano-silica extracted from natural sources. In the present, silica is extracted from several natural sources such as corn cob, sugarcane bagasse ash, bamboo, rice straw, rice husk ash, and others. The preparation of silica using rice husk ash (RHA) is an interesting approach because normally it contains a high silica content of over 60%. Furthermore, RHA is the by-product of the process of rice husk (RH) pyrolysis for energy production, which is usually dumped in landfills, leading to air and water pollution. To reduce this issue and increase the value of this material, the current use of RHA is in many applications such as fertilizer, adsorbent and catalyst in the form of activated carbon or silica, and in the cement and concrete industries in the form of silicate or silica, etc. (Pode, 2016; Shen, 2017; Shen et al., 2014).

2.4 Preparation of silica from rice husk ash

There are several methods to extract silica from RHA, including heat, lye, sol-gel, and precipitation (Guo et al., 2021). The precipitation method is popular because it is simple, economical, and repeatable. To obtain silica, the main conventional procedure is to first extract it using alkali and then precipitate it using acid (Yuvakkumar et al., 2014).

Thuadaij & Nuntiya (2008) prepared the nano-silica from RHA by the precipitation method. First, the sodium hydroxide (NaOH) solution was used to extract silica from RHA for 3 hours. The solution was filtered to obtain the sodium silicate solution. The 5N sulfuric acid (H_2SO_4) was added to the sodium silicate solution until the pH reached 2, and then ammonium hydroxide (NH_4OH) was added to the previous solution until the pH reached 8.5. The solution was left for 3.5 hours. The pure silica was filtered from the previous solution and dried at 120°C for 12 hours. In this study, the optimal condition to prepare pure silica is to use RHA that has been calcined at 700°C for 6 hours as the raw material and a 2.5N NaOH solution to extract silica. Then, the pure silica was extracted by refluxing with 6N hydrochloric acid (HCl) for 4 hours and washing it with deionized (DI) water to make the acid free. The pure silica was dissolved in 2N NaOH solution by stirring for 10 hours, and then H_2SO_4 was added to adjust the pH of the solution in the range of 7.5-8.5. The nano-silica was washed with warm DI water to make it alkali free and dried at 50°C for 48 hours. The prepared nano-silica showed an agglomerate form with a diameter of about 50 nm and a specific area of 656 m^2/g. Moreover, the prepared nano-silica was found to have a typical amorphous form.

Majumder et al. (2014) prepared the amorphous silica from RHA by the precipitation method. First, the collected RH was sieved to remove dust, washed with DI water to remove impurities of soil and dust, and dried at 60°C for 24 hours. Then, the dried RH was calcined at 450°C for 15 minutes to obtain the RHA. The RHA was washed with DI water, dried in hot-air oven for 24 hours, and crushed to a size of 300 micrometers. Then, the RHA was washed with 2M HCl for 2 hours to remove mineral impurities and the residue of RHA was filtered. The filtered residue was washed with

DI water and dried at 60°C for 24 hours. Then, the silica was extracted from the previous RHA using a 1M NaOH solution at 80°C for 2 hours and filtered the residue of unreacted RHA to obtain the sodium silicate solution. Then, the sodium silicate solution was titrated with 2M HCl to adjust the pH of the solution in the range of 7-10 and aged for 24 hours to form silica gel. The DI water was added to silica gel and stirred to make a slurry solution. The slurry solution was centrifuged at 6,000 rpm for 15 minutes to obtain the separated solid gel, washed with DI water, and dried at 80°C for 12 hours to obtain the silica. The prepared silica was found to have a typical amorphous form with a silica content greater than 90%.

Dhaneswara et al. (2020) prepared the silica from RHA by the precipitation method. The RHA was calcined at 700°C for 5 hours to obtain the RHA that is used as the raw material. The silica was extracted from RHA using 5% or 10% NaOH solution at 80°C for 1 hour and the residue of unreacted RHA was filtered out to obtain the sodium silicate solution. Then, the 1M HCl or acetic acid (CH_3COOH) was titrated into the sodium silicate solution to a pH of 7, which forms the silica gel. The previous gel was filtered and dried at 120°C for 12 hours. Then, the silica was washed with DI water at 80°C for 15 minutes to dissolve any salts that might form, filtered, and dried at 120°C for 4 hours. All the prepared silica was found to have a typical amorphous form with a purity of 98-99%. In this study, the silica extracted from 10% NaOH and precipitated using HCl had the largest surface area.

However, it is known that silica and NR are generally incompatible due to the polarity and non-polarity of materials. Thus, to improve the functionality of materials, using vinyltriethoxysilane (VTES) as a compatibilizer or XSBR combined in the systems may reduce this issue. The chemical structures of VTES and XSBR are shown in Figures 2.5 and 2.6, respectively.

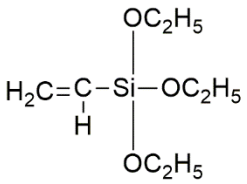

Figure 2.5 Chemical structure of VTES.

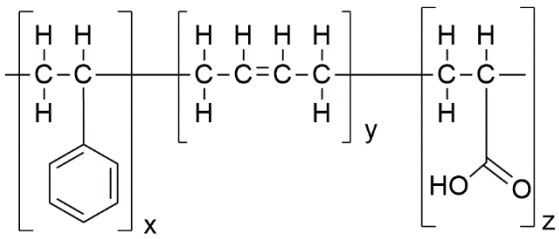

Figure 2.6 Chemical structure of XSBR.

CHAPTER 3
RESEARCH METHODOLOGY

3.1 Materials

Natural rubber latex (NRL) treated with high ammonia and content of dry rubber at 60wt% was purchased from Chemical & Materials Co., Ltd. Carboxylated styrene-butadiene latex (XSBRL) was purchased from Jorakay Corporation Co., Ltd. Commercial sodium silicate (CSS) was purchased from PanReac AppliChem ITW Reagents. Rice husk ash (RHA) that is by-product from biomass power plants was purchased from Chia Meng Co., Ltd. Hydrochloric acid (HCl) was purchased from RCI Labscan Co., Ltd. Sodium hydroxide (NaOH) and acetic acid (CH_3COOH) were purchased from CARLO ERBA Reagents. Vinyltriethoxysilane (VTES) was purchased from Sigma-Aldrich Co., Ltd. Stearic acid (SA), zinc oxide (ZnO), N-Cyclohexyl-2-benzothiazole sulfenamide (CBS), and sulfur (S) were supported by Chemical Innovation Co., Ltd. Portland cement Type I was produced by Asia Cement Pub Co., Ltd. Sodium dodecyl sulfate (SDS) was purchased from LOBA Chemie Pvt. Ltd. Sand with a particle size less than 1.18 mm was supported by Concrete Technology Laboratory at Suranaree University of Technology.

3.2 Experimental

3.2.1 Preparation of RSi and CSi

3.2.1.1 Extraction of rice husk sodium silicate (RSS)

The RHA was purified by leaching RHA with 1M HCl solution at 90°C by using magnetic stirrer for 3 hours to remove some metallic oxides. Then the purified RHA was filtered by using filter paper, washed with DI water until the pH was neutral, and dried by using hot-air oven at 110°C for 12 hours. The RSS was prepared by extracting silica from the purified RHA that was obtained from the previous process with 1M NaOH solution at 90°C. The purified RHA was stirred by using magnetic stirrer

for 12 hours to obtain the yield of silica about 68%. And then the filter paper was utilized to filter the residue of purified RHA and obtain the RSS with clear solution.

3.2.1.2 Precipitation of RSi and CSi

The RSi was prepared by precipitating silica in RSS with 1M CH_3COOH solution at room temperature under stirring on over-head stirrer throughtout the process. The CH_3COOH solution was dropped into RSS until the pH was neutral to obtain the RSi. The CSi was also prepared by following from the previous process.

3.2.2 Characterization of RSi and CSi

Before characterization, the RSi and CSi were washed with DI water several times and filtered by using filter paper. Then the prior RSi and CSi were dried by using hot-air oven at 110°C for 12 hours and grounded by using mortar to obtain the dried RSi and CSi with fine particles.

3.2.2.1 Fourier transform infrared spectrometer (FTIR)

The functional groups of dried RSi and CSi were analyzed by using the FTIR (Bruker, TENSOR 27) in wavenumber range of 4000 to 400 cm^{-1} with resolution of 4 cm^{-1} and number of scans of 64. All the samples were mixed with potassium bromide (KBr) by using agate mortar and pressed into pellets to obtain the test specimens with smooth surface for transmittance measurements.

3.2.2.2 Energy dispersive X-Ray fluorescence spectrometer (EDXRF)

The EDXRF (HORIBA Scientific, XGT-5200) was used to analyze the chemical compositions of dried RSi and CSi.

3.2.2.3 X-Ray diffractometer (XRD)

The XRD diffractograms of dried RSi and CSi were analyzed by using the XRD (Bruker, D2 PHASER) in 2θ range of 10 to 70 degrees.

3.2.2.4 Branauer-Emmett-Teller (BET) analysis

The characteristics of dried RSi and CSi in terms of BET surface area, total pore volume, and average pore diameter were analyzed by using the BET method (Micromeritics, ASAP 2020). All the samples were degassed at 160°C for 24 hours before analysis.

3.2.2.5 Dynamic light scattering (DLS) measurement

The average particle sizes of RSi and CSi were measured by using the DLS (Malvern Panalytical, Zetasizer Nano ZS). All the samples were dispersed in ethanol by using an ultrasonic probe before the measurement.

3.2.2.6 Field Emission Scanning Electron Microscope (FESEM)

For this characterization, the RSi and CSi were dispersed in ethanol by using an ultrasonic probe. Then the prior RSi and CSi were dropped on the aluminum tape and allowed to dry overnight in the electronic desiccator.

The images of dried RSi and CSi were acquired using FESEM (Carl Zeiss, AURIGA). All the samples were coated with carbon before the observation.

3.2.3 Preparation of rubber composite

3.2.3.1 Mixing and drying of rubber sheet

1) NR/RSi sheet

The RSi at 0, 5, 10, and 20 phr was poured into NRL and mixed by using over-head stirrer at room temperature for 15 minutes to obtain the mixture. Then each prior mixture was poured onto tray and dried by using hot-air oven at 60°C for 72 hours to obtain the NR/RSi sheet with constant weight.

2) NR/VTES/RSi sheet

First, the RSi at 0, 5, 10, and 20 phr was combined with VTES by dropping VTES into RSi at a ratio of 1/10, which was the optimal ratio of VTES onto RSi. The previous process was prepared by using over-head stirrer at room temperature for 15 minutes. Then the prior product was poured into NRL and mixed by using over-head stirrer for 15 minutes to obtain the mixture. And then the NR/VTES/RSi sheet was prepared by pouring each mixture onto tray and drying in a hot-air oven at 60°C for 72 hours.

3) NR/XSBR/RSi sheet

First, the NRL was blended with XSBRL at a ratio of 2/1, which was the optimal blending ratio of NRL with XSBRL. The homogeneous rubber latex blend was prepared by using over-head stirrer for 15 minutes. Then the rubber latex blend was mixed with RSi at 0, 5, 10, and 20 phr for 15 minutes under stirring on over-

head stirrer to obtain the mixture. And then each mixture was poured onto tray and dried by using hot-air oven at 60°C to obtain the NR/XSBR/RSi sheet with constant weight.

3.2.3.2 Compounding and vulcanizing of rubber composite

All the rubber sheets were compounded with chemicals that were shown in Table 3.1. The two-roll mill was used to compound each rubber sheet with chemicals for 15 minutes to obtain the rubber compound. Then each prior rubber compound was vulcanized by using compression molding machine at 150°C with an optimal curing time that was determined by using a moving die rheometer (MDR) to obtain the rubber composite.

Table 3.1 Rubber compounding chemicals.

Chemical	Function	Content (*phr)
Stearic acid (SA)	Activator	2
Zinc oxide (ZnO)	Activator	5
N-cyclohexyl-2-benzothiazole sulfonamide (CBS)	Accelerator	2.5
Sulfur (S)	Crosslinking agent	1

*phr refers to part per hundred of rubber.

3.2.4 Characterization of rubber composite

3.2.4.1 Cure characteristics

The cure characteristics such as minimum torque, maximum torque, scorch time, and optimal cure time of rubber composites were determined by using a MDR (GOTECH, M-2000AN) according to ASTM D2084 with a temperature of 150°C.

3.2.4.2 Mechanical properties

The modulus at 100% elongation (M100), modulus at 300% elongation (M300), tensile strength, and percentage of elongation at break of rubber composites were measured according to ASTM D412 with the type C test specimen,

as shown in Figure 3.1, by using a universal testing machine (UTM, INSTRON, Model:5565) with a load cell of 5 kN and crosshead speed of 500 mm/min.

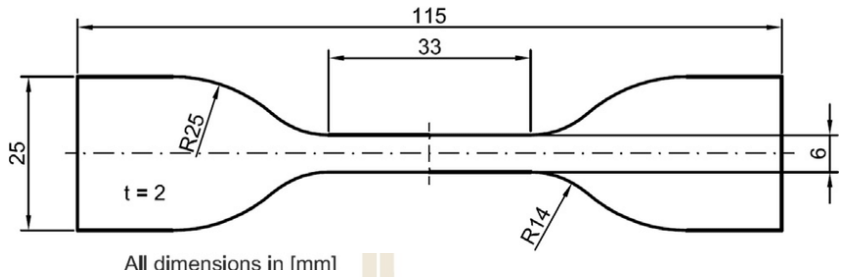

Figure 3.1 Dimensions of the type C test specimen according to ASTM D412 (Staudt et al., 2018).

The hardness of rubber composites were measured according to ASTM D2240 by using a hardness tester (Bareiss, HPE II) with the Shore A test method.

3.2.4.3 Morphological properties

The secondary electron images of rubber composites were acquired using a FESEM (Carl Zeiss, AURIGA). The tensile fracture surfaces of rubber composites were coated with gold before the observation.

3.2.5 Preparation of polymer-modified mortar (PMM)

The sample codes and mixing proportions of PMM are listed in Table 3.2. The ratios of cement to sand (C/S), water to cement (W/C), and SDS to polymer (SDS/P) were fixed at 0.50, 0.55, and 0.10, respectively. The polymer was added to cement at a polymer to cement (P/C) ratio of 0.00, 0.05, 0.10, and 0.20. All the samples were mixed according to ASTM C305 by using mortar mixer at room temperature. The mixing procedures are as follows:

1) Place all the mixing water in the bowl.

2) Add the cement to the water then start the mixer and mix at the slow speed of 140 rpm for 30 seconds.

3) Add the entire quantity of sand slowly over 30 seconds period, while mixing at slow speed of 140 rpm.

4) Stop the mixer, change to medium speed of 285 rpm and mix for 30 seconds.

5) Stop the mixer and let the mortar stand for 90 seconds. During the first 15 seconds of this interval, quickly scrape down into the batch any mortar that may have collected on the side of the bowl.

6) Finish by mixing for 60 seconds at medium speed of 285 rpm.

Then the fresh mortars were cast in molds and allowed to harden for 1 day. The prior hardened mortars were demolded and immersed in tap water for curing, as shown in Figure 3.2. The curing time of all the samples was fixed at 28 days. Then the cured mortars were taken out of the tap water and allowed to dry at room temperature for 3 hours to obtain the PMM without water on the surface.

Figure 3.2 Curing of the test specimens.

Table 3.2 Sample codes and mix proportions of PMM.

Sample	C/S	W/C	SDS/*P	*P/C
Unadded PMM	0.50	0.55	-	-
0.05PMM	0.50	0.55	0.10	0.05
0.10PMM	0.50	0.55	0.10	0.10
0.20PMM	0.50	0.55	0.10	0.20

*P refers to the mixture of 2NR/XSBR/5RSi.

3.2.6 Characterization of polymer-modified mortar (PMM)

3.2.6.1 Mechanical properties

1) Tensile properties

The PMM specimens with a briquette-shape were used to test in tension mode according to ASTM C190 by using flexural/tensile testing machine (ELE International) with a load of 10 kN. Figure 3.3 represents the dimensions of briquette-shape test specimen according to ASTM C190.

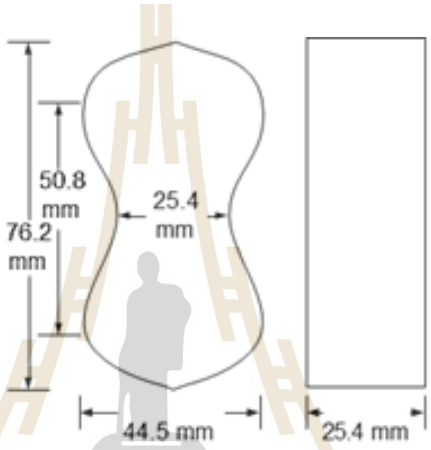

Figure 3.3 Dimensions of the briquette-shape test specimen according to ASTM C190 (https://www.lceted.com/2021/08/laboratory-tests-on-cement.html).

2) Compressive properties

The cube specimens of PMM with dimensions of 50 x 50 x 50 mm were used to test in compression mode according to ASTM C109 by using a semi-automatic compression machine (ELE International, ADR Touch SOLO 2000) with a pace of 100 kN/s. The equation that was used to calculate the tensile strength and compressive strength of PMM is:

$$S_T \; or \; S_C \; = \frac{P}{A}$$

Where:

S_T or S_C = tensile strength or compressive strength (MPa),

P = total maximum load (N), and

A = area of loaded surface (mm^2).

3) Flexural properties

The PMM specimens with a prism shape in dimensions of 40 x 160 x 40 mm were used to test in flexure mode according to ASTM C348 by using flexural/tensile testing machine (ELE International) with a load of 10 kN. The flexural strength of PMM was calculated by following the equation:

$$S_F \; = \; 0.0028P$$

Where:

S_F = flexural strength (MPa), and

P = total maximum load (N).

3.2.6.2 Water absorption

Before this characterization, the cube specimens of PMM with dimensions of 50 x 50 x 50 mm were dried in a hot-air oven at 110°C for 24 hours. Then the dried PMM specimens were allowed to cool at room temperature for 3 hours to obtain the PMM specimens with ambient temperature surfaces.

The water absorption of PMM was measured according to ASTM C1403. The PMM specimens were immersed in tap water for different immersion times of 0.25, 1, 4, and 24 hours. The equation that was used to calculate the water absorption of PMM is:

$$A_t = (W_t - W_0) \times \frac{10000}{(L_1 \times L_2)}$$

Where:

A_t = the water absorption (g/100 cm^2),

W_t = the weight of the specimen at time t (g),

W_0 = the initial weight of the specimen (g),

L_1 = the average length of the test surface of the mortar specimen cube (mm), and

L_2 = the average width of the test surface of the mortar specimen cube (mm).

3.2.6.3 Morphological properties

The images of PMM were acquired using a FESEM (Carl Zeiss, AURIGA). The compressive fracture surfaces of PMM were coated with gold before the observation.

CHAPTER 4
RESULTS AND DISCUSSION

4.1 Characterization of RSi and CSi

In this section, the RSi that was prepared from RHA is compared with CSi in terms of chemical and physical properties.

4.1.1 Fourier transform infrared spectrometer (FTIR)

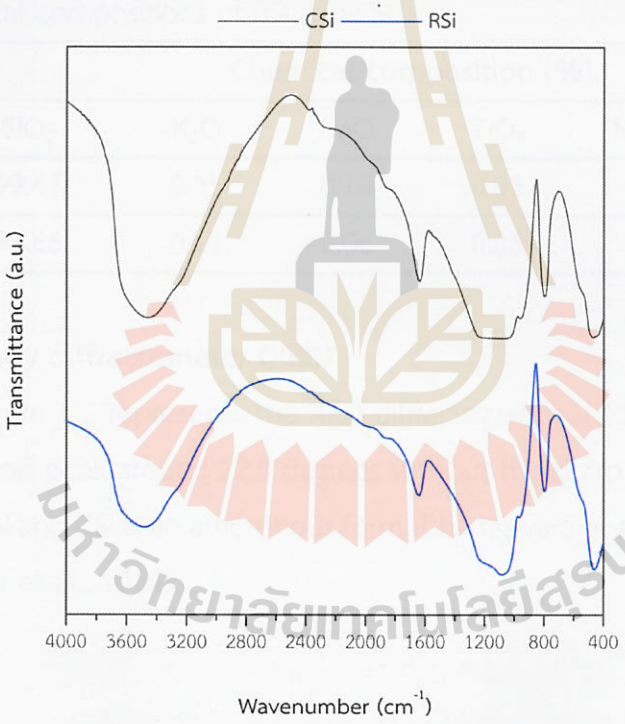

Figure 4.1 FTIR spectra of RSi and CSi.

The functional groups of RSi and CSi are shown in Figure 4.1. The FTIR spectra of RSi and CSi show a broad band between 2850 and 3800 cm^{-1} corresponds to the -OH stretching vibration of silanol groups and adsorbed water. The band at 1630 cm^{-1} corresponds to the -OH bending vibration of silanol groups. The band between 1050 and 1250 cm^{-1} corresponds to the asymmetric stretching vibration of siloxane

groups. The bands at 470 and 798 cm^{-1} correspond to the asymmetric bending and symmetric stretching vibrations of siloxane groups (Azat et al., 2019; Dhaneswara et al., 2020; Dung et al., 2017; Jembere & Fanta, 2017; Yuvakkumar et al., 2014). This indicates that the RSi prepared from RHA has functional groups resembling the CSi.

4.1.2 Energy dispersive X-ray fluorescence spectrometer (EDXRF)

The chemical compositions of RSi and CSi are listed in Table 4.1. The RSi shows the percentage of chemical compositions that are similar to the CSi, which contains SiO_2 composition percentage of approximately 99. This indicates the RHA can prepare RSi with a purity equivalent to the CSi.

Table 4.1 Chemical compositions of RSi and CSi.

Sample	Chemical composition (%)					
	SiO_2	K_2O	CaO	TiO_2	MnO_2	Fe_2O_3
RSi	99.47	0.35	0.10	0.03	-	0.05
CSi	99.66	0.11	0.06	0.06	-	0.11

4.1.3 X-ray diffractometer (XRD)

Figure 4.2 represents the XRD diffractograms of RSi and CSi that only observed the broad peak around 22.5 degrees without the sharp peak, indicating the typical form of RSi and CSi is an amorphous form (Dhaneswara et al., 2020; Dung et al., 2017; Yuvakkumar et al., 2014).

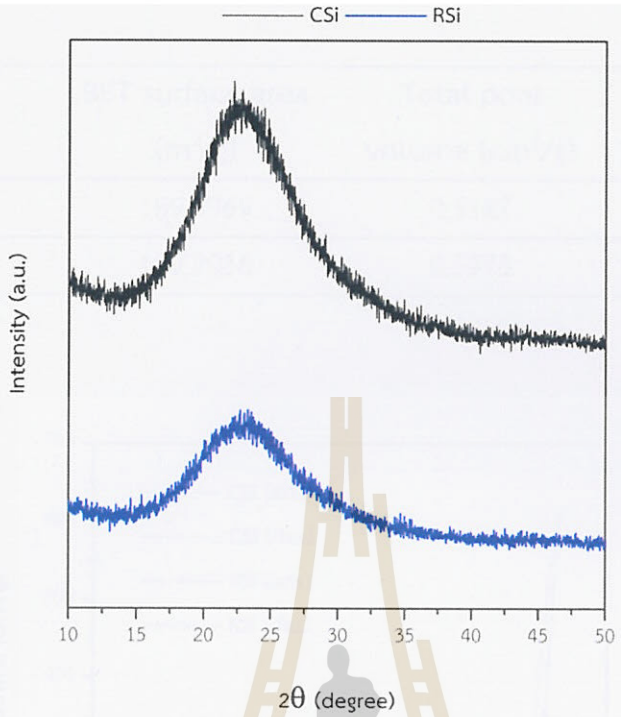

Figure 4.2 XRD diffractograms of RSi and CSi.

4.1.4 Branauer-Emmett-Teller (BET) analysis

The BET surface area, total pore volume, and average pore diameter of RSi and CSi are listed in Table 4.2. The RSi and CSi show the average pore diameter of approximately 6.7 and 18.5 nm, respectively. In addition, the RSi shows a BET surface area of approximately 190 m^2/g that is higher than the BET surface area of CSi, which has a BET surface area of approximately 129 m^2/g. Furthermore, the physisorption isotherms of RSi and CSi are shown in Figure 4.3. The RSi shows the physisorption isotherm is a type IVa that occurs for pores wider than 4 nm, which relates to the result of the average pore diameter of RSi that is listed in Table 4.2. For the CSi, the physisorption isotherm is a type II with a type H3 hysteresis loop that occurs for slit-shaped pores (Dhaneswara et al., 2020; Thommes et al., 2015).

Table 4.2 BET surface are, total pore volume, and average pore diameter of RSi and CSi.

Sample	BET surface area (m^2/g)	Total pore volume (cm^3/g)	Average pore diameter (nm)
RSi	189.9969	0.3187	6.7097
CSi	129.2036	0.5975	18.4975

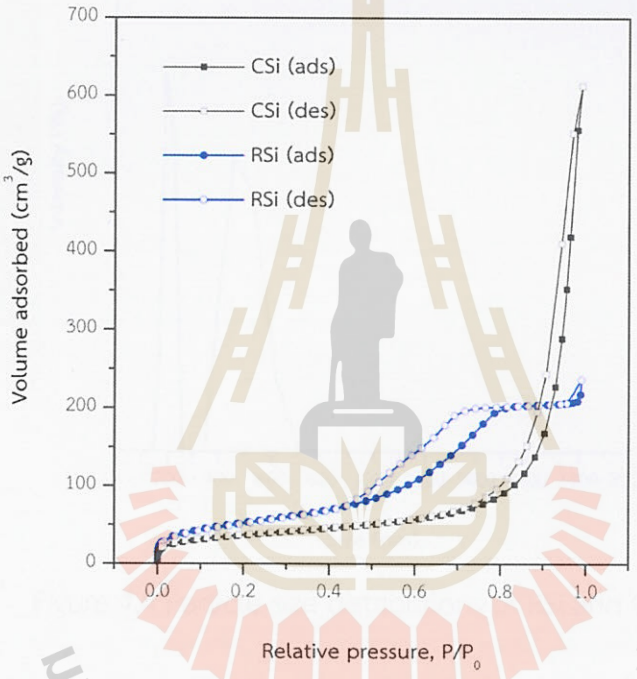

Figure 4.3 Physisorption isotherms of RSi and CSi.

4.1.5 Dynamic light scattering (DLS) measurement

The average particle sizes of RSi and CSi are listed in Table 4.3 and the particle size distributions of RSi and CSi are shown in Figure 4.4. The RSi shows an average particle size of approximately 190 nm that is smaller than the average particle size of CSi, which has an average particle size of approximately 459 nm.

Table 4.3 Average particle sizes of RSi and CSi.

Sample	Average particle size (nm)
RSi	190.14
CSi	458.67

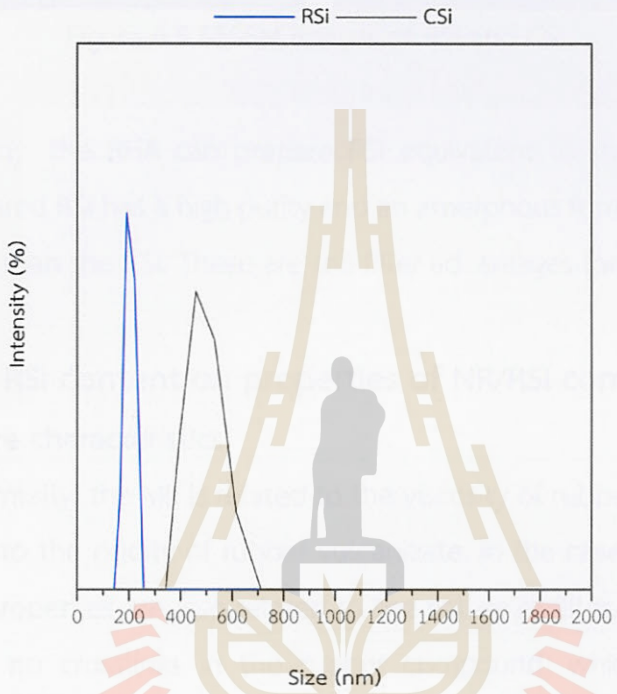

Figure 4.4 Particle size distributions of RSi and CSi.

4.1.6 Field emission scanning electron microscope (FESEM)

The FESEM images of RSi and CSi that were observed at a magnification of 50,000x are shown in Figure 4.5. The images of RSi and CSi show their particles in a spherical shape. Where the CSi image clearly shows the CSi particle boundary more than the RSi particle because the RSi particle is smaller, making the particle more agglomerate. Moreover, the particle size observed with an electron microscope was found to be smaller than the particle size measured by DLS. This is similar to the results of material size reported in several reports (Kato et al., 2014; Kobler et al., 2008; Thiele et al., 2010).

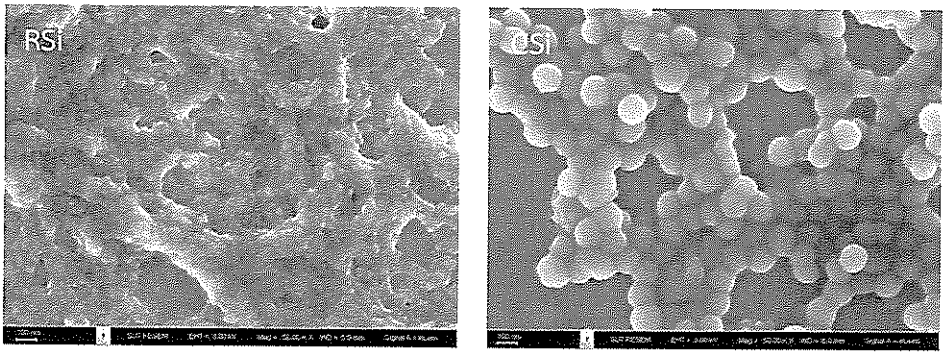

Figure 4.5 FESEM images of RSi and CSi.

In this study, the RHA can prepare RSi equivalent to the properties of CSi because the prepared RSi has a high purity and an amorphous form. Moreover, the RSi has a smaller size than the CSi. These are the filler advantages for use in rubber.

4.2 Effect of RSi content on properties of NR/RSi composites

4.2.1 Cure characteristics

Normally, the ML is related to the viscosity of rubber compound, while the MH is related to the rigidity of rubber vulcanizate. In the case of the filler added to rubber, these properties are also related to the nature of filler. In addition, the ts2 is the time with no crosslinks in the rubber compound, which is an important parameter for the safe processing of rubber in molds. The tc90 is another important parameter that determines the time required to produce the rubber products (Balan et al., 2017; Bureewong et al., 2023; Inphonlek et al., 2022; Nihmath & Ramesan, 2020; Nihmath & Ramesan, 2021; Rabiei & Shojaei, 2016; Srisuwan et al., 2018).

The cure characteristics in terms of ML, MH, ts2, tc90, and cure rate index of NR and NR/RSi composites are summarized in Table 4.4. The ML and MH of NR and NR/RSi composites are displayed in Figure 4.6a and the ts2 and tc90 of NR and NR/RSi composites are displayed in Figure 4.6b. The addition of RSi to NR increased the ML of NR and further increased with increasing RSi content. Because the presence of silica particles in the rubber matrix restricts the mobility of rubber chains, the viscosity of rubber compound increases (Boonmee & Jarukumjorn, 2020). In terms of ts2 and tc90, the addition of RSi to NR decreased these properties. Because the presence of sodium acetate generated from the RSi preparation acts as a catalyst, the

time required to vulcanize the rubber composites decreases (de Paiva et al., 2019). This may be one of the advantages of using RSi as a filler in NR because the addition of RSi to NR can reduce the tc90 of NR, allowing the product to be obtained in a shorter time. Moreover, the increment of RSi content in the NR composite, the ts2 and tc90 tend to slightly increase and decrease, respectively. Because the silica surface adsorbs accelerator, the ts2 of the compound increases and the system of filled NR with increasing RSi content becomes more heated from the filler friction, which affects the increased degree of curing. For the MH, the addition of RSi to NR has no effect on this property.

Table 4.4 Cure characteristics of NR and NR/RSi composites.

Sample	ML (dNm)	MH (dNm)	ts2 (sec)	tc90 (sec)	Cure rate index (sec^{-1})
NR	4.51	25.54	159	254	1.05
NR/5RSi	6.61	25.61	80	148	1.47
NR/10RSi	9.28	25.27	89	142	1.89
NR/20RSi	11.73	25.55	92	140	2.08

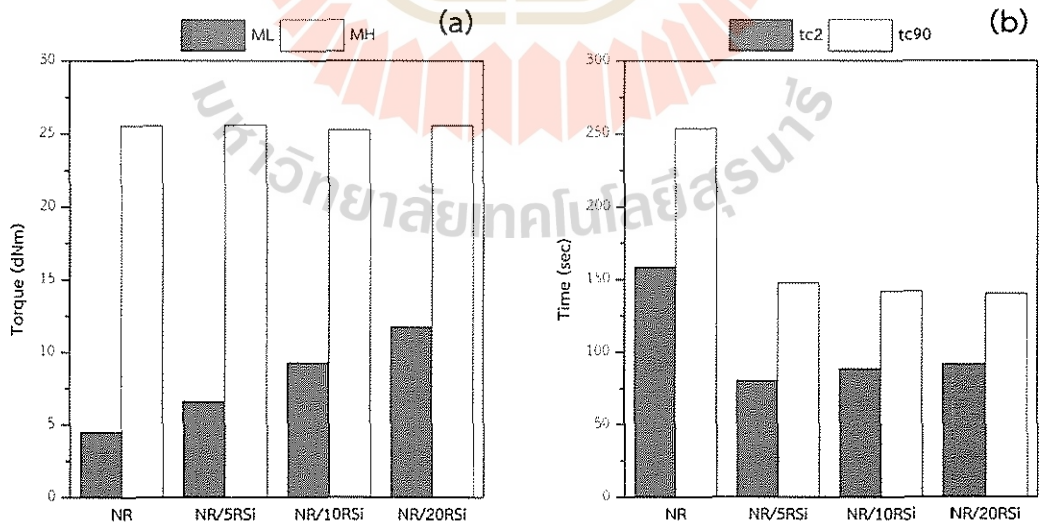

Figure 4.6 Cure characteristics of NR and NR/RSi composites showing (a) ML and MH and (b) t2 and tc90.

4.2.2 Mechanical properties

The mechanical properties in terms of M100, M300, tensile strength, elongation at break, and hardness of NR and NR/RSi composites are summarized in Table 4.5. The M100 and M300 of NR and NR/RSi composites are displayed in Figure 4.7a. The addition of RSi to NR increased the M100 and M300 of NR. Because the fact that filler with a higher stiffness than the matrix can increase the modulus of composite (Boonmahitthisud & Chuayjuljit, 2012; Bureewong et al., 2022a; Bureewong et al., 2022b). This is the reason for the increase in the M100 and M300 of NR. While the increment of RSi content in the NR composite, the M100 and M300 show an insignificant increase. These properties show the same trend as the hardness properties of NR and NR/RSi composites, which are shown in Figure 4.7d. The tensile strength and elongation at break of NR and NR/RSi composites are displayed in Figures 4.7b and 4.7c, respectively. The addition of RSi to NR increased the tensile strength of NR and further increased with increasing RSi content. For the elongation at break, the addition and increment of RSi content in the NR matrix tend to slightly increase. This is interesting because in the normal case, the addition of silica to NR results in a decrease in the elongation at break. Thus, the addition of RSi to NR improves the mechanical properties, especially its tensile strength. Where the highest tensile strength value of NR/RSi composite is the addition of RSi at 20 phr.

Table 4.5 Mechanical properties of NR and NR/RSi composites.

Sample	M100 (MPa)	M300 (MPa)	Tensile strength (MPa)	Elongation at break (%)	Hardness (Shore A)
NR	0.65 ± 0.01	1.56 ± 0.03	7.18 ± 0.79	688.03 ± 34.27	26.70 ± 0.10
NR/5RSi	0.78 ± 0.08	1.79 ± 0.16	12.34 ± 1.84	715.19 ± 9.16	32.78 ± 0.62
NR/10RSi	0.89 ± 0.04	2.09 ± 0.12	17.65 ± 1.42	730.56 ± 15.93	34.80 ± 1.48
NR/20RSi	1.07 ± 0.16	2.59 ± 0.47	20.86 ± 0.96	760.55 ± 53.63	38.82 ± 1.39

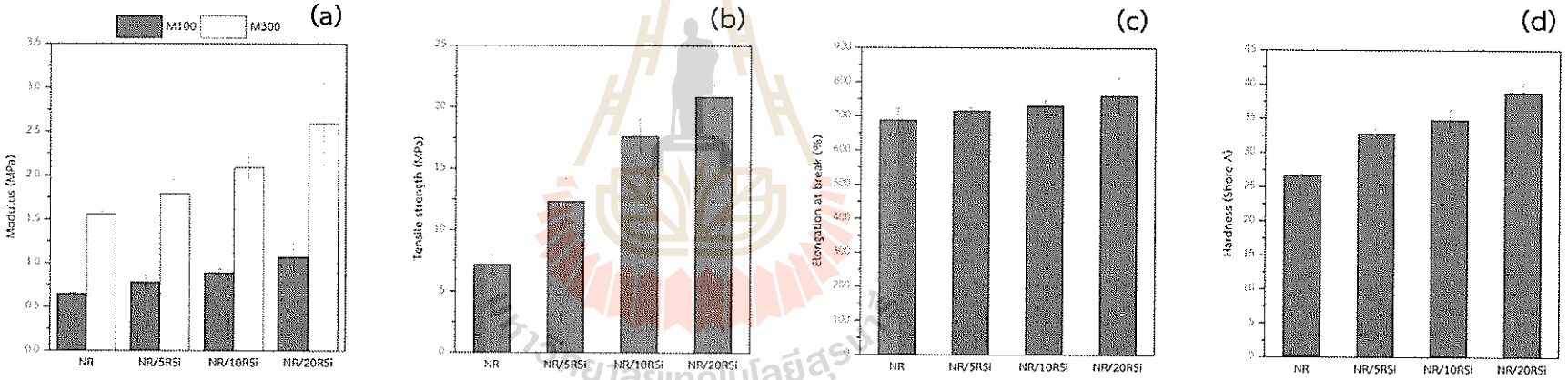

Figure 4.7 Mechanical properties of NR and NR/RSi composites showing (a) M100 and M300, (b) tensile strength, (c) elongation at break, and (d) hardness.

4.2.3 Morphological properties

In general, the morphological properties of polymer composites are necessary to report in order to understand the dispersion, compatibility, and characteristics of filler after the mixing and forming processes (Balan et al., 2017; Bureewong et al., 2023; Nihmath & Ramesan, 2017; Nihmath & Ramesan, 2018).

Figure 4.8 FESEM images and EDS mapping of fractured NR and NR/RSi composites.

The FESEM images and EDS mapping of fractured NR and NR/RSi composites are shown in Figure 4.8. The tensile fracture surface of NR shows a smooth surface without the Si element on the surface. On the other hand, the tensile fracture surface of NR/RSi composite shows the dispersion and agglomeration of RSi particles on the surface. Where the agglomeration of RSi particles increased with increasing RSi content. This relates to the results of the EDS mapping of NR/RSi composites, which observed that the concentration and agglomeration of Si elements increased with increasing RSi content. Furthermore, the addition of RSi to NR increased the roughness of the tensile fracture surface of NR and further increased with increasing RSi content. Normally, the roughness of the fracture surface indicates that the sample failed in a ductile manner (Boonmahitthisud et al., 2017). This relates to the fact that the elongation at break of NR/RSi composites tends to slightly increase with increasing RSi content, indicating the RSi is an effective reinforcement filler for NR, although the RSi exhibits non-uniform dispersion and some agglomeration.

4.3 Effect of RSi content on properties of NR/VTES/RSi composites

First, the RSi at a content of 5 phr was used to find the optimal ratio of VTES/RSi by dropping VTES into 5RSi at the contents of 0.5, 1.0, and 2.0 phr before mixing with the NRL. Then drying, compounding, and vulcanizing to obtain the NR/VTES/5RSi composite. After that, the composites were tested in terms of mechanical properties.

The mechanical properties in terms of M100, M300, tensile strength, elongation at break, and hardness of NR/5RSi and NR/VTES/5RSi composites are summarized in Table 4.6. The mechanical properties of NR/VTES/5RSi composite showed a higher value than those of NR/5RSi composite because of the formation of chemical bonds between NR and VTES/RSi, as illustrated in Figure 4.10, which improve the interaction between NR and VTES/RSi better than the interaction between NR and RSi (Yin et al., 2019). However, the mechanical properties of NR/VTES/5RSi composites trended to slightly decrease with increasing VTES content. This is because the excess VTES content generates the polarity form that is the weak point in the NR/VTES/5RSi composite. Thus, the optimal ratio of VTES/RSi is 1/10.

Table 4.6 Mechanical properties of NR/5RSi and NR/VTES/5RSi composites.

Sample	M100 (MPa)	M300 (MPa)	Tensile strength (MPa)	Elongation at break (%)	Hardness (Shore A)
NR/5RSi	0.78 ± 0.08	1.79 ± 0.16	12.34 ± 1.84	715.19 ± 9.16	32.78 ± 0.62
NR/0.5VTES/5RSi	0.86 ± 0.03	2.01 ± 0.05	14.76 ± 0.97	729.24 ± 29.23	35.00 ± 0.39
NR/1.0VTES/5RSi	0.83 ± 0.02	1.93 ± 0.05	13.95 ± 0.63	722.41 ± 7.36	34.66 ± 0.28
NR/2.0VTES/5RSi	0.83 ± 0.01	1.92 ± 0.03	13.45 ± 0.70	714.57 ± 11.04	33.94 ± 0.34

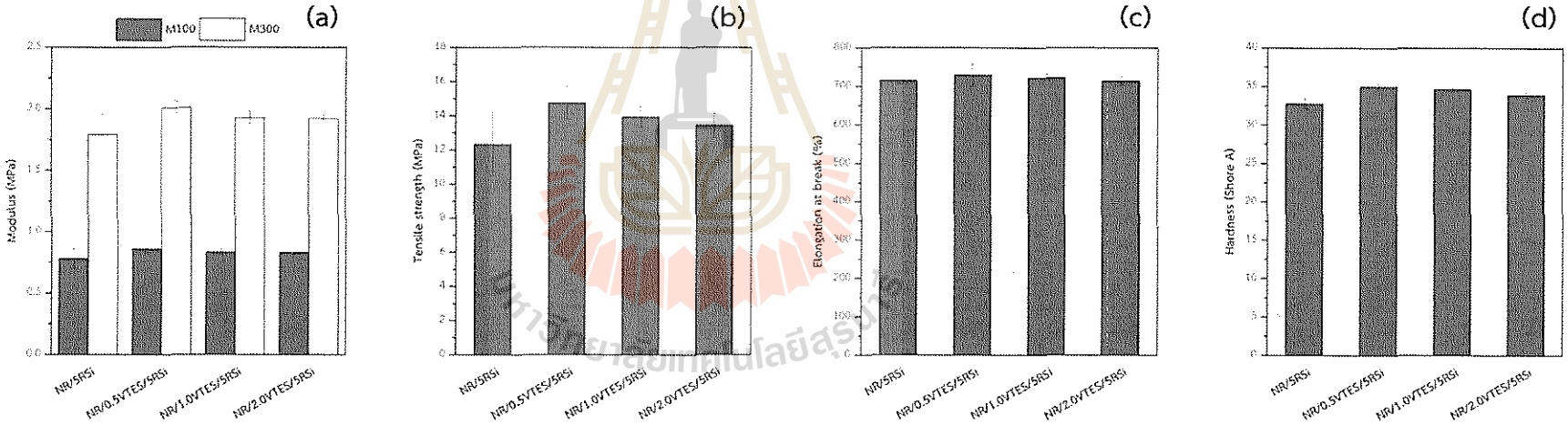

Figure 4.9 Mechanical properties of NR/5RSi and NR/VTES/5RSi composites showing (a) M100 and M300, (b) tensile strength, (c) elongation at break, and (d) hardness.

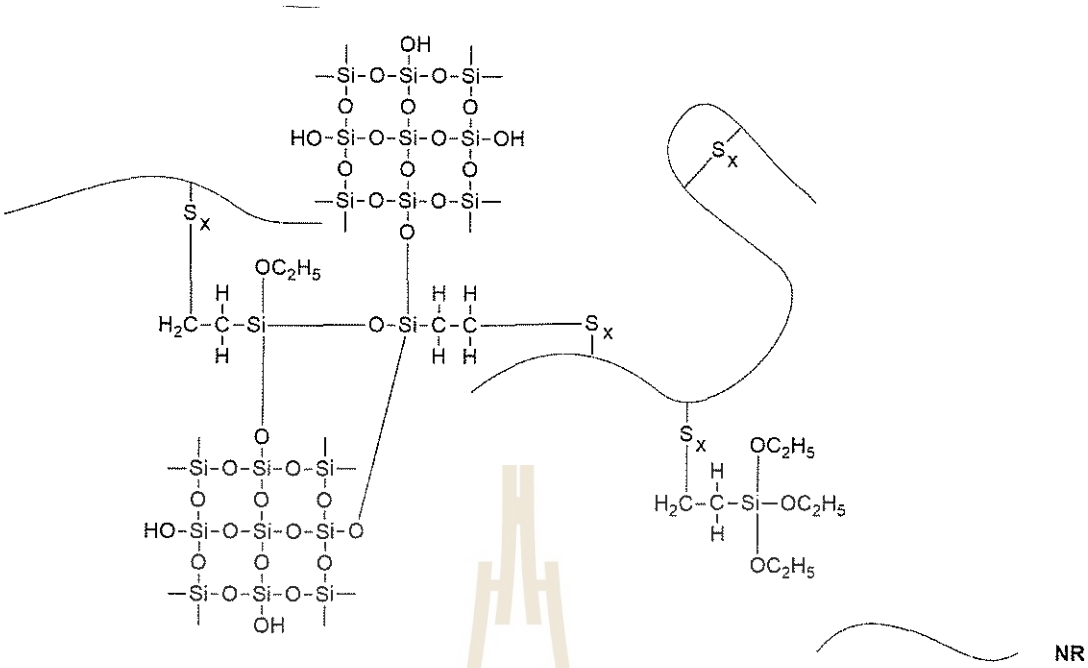

Figure 4.10 Chemical bonding of NR/VTES/RSi composite.

4.3.1 Cure characteristics

The cure characteristics in terms of ML, MH, ts2, tc90, and cure rate index of NR and NR/VTES/RSi composites are summarized in Table 4.7. The ML and MH of NR and NR/VTES/RSi composites are displayed in Figure 4.11a. The addition of VTES/RSi to NR increased the ML and MH of NR because the presence of silica particles in the rubber matrix increases the viscosity of rubber compound and the stiffness of silica increases the rigidity of composite vulcanizate (Boonmee & Jarukumjorn, 2020). However, the increment of VTES/RSi content in the NR matrix has no effect on the ML and MH of NR/VTES/RSi composites. The ts2 and tc90 of NR and NR/VTES/RSi composites are displayed in Figure 4.11b. The addition of VTES/RSi to NR decreased the ts2 and tc90 of NR because the presence of sodium acetate generated from the RSi preparation acts as a catalyst (de Paiva et al., 2019). Moreover, the increment of VTES/RSi content in the NR matrix, the ts2 and tc90 tend to slightly increase and decrease, respectively. Because the silica surface adsorbs accelerator, the ts2 of the compound increases and the system of filled NR with increasing RSi content becomes more heated from the filler friction, which affects the increased degree of curing.

Table 4.7 Cure characteristics of NR and NR/VTES/RSi composites.

Sample	ML (dNm)	MH (dNm)	ts2 (sec)	tc90 (sec)	Cure rate index (sec^{-1})
NR	4.51	25.54	159	254	1.05
NR/0.5VTES/5RSi	5.64	27.67	78	158	1.25
NR/1.0VTES/10RSi	5.46	27.44	81	152	1.41
NR/2.0VTES/20RSi	5.79	27.11	88	148	1.67

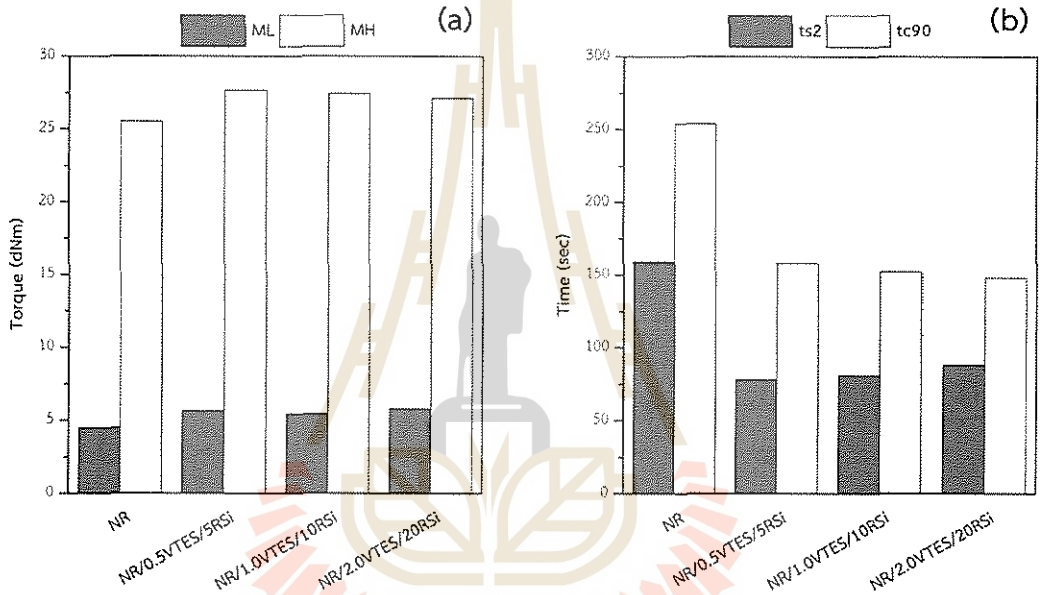

Figure 4.11 Cure characteristics of NR and NR/VTES/RSi composites showing (a) ML and MH and (b) t2 and tc90.

4.3.2 Mechanical properties

It is well known that the characteristics and dispersion of filler are directly related to the properties of polymer composite. Additionally, the area under the stress-strain curves is related to the toughness of polymer. In general, the mechanical properties depend on the nature of filler, dispersion, and the interaction between filler and polymer matrix (Akbay et al., 2018; Bureewong et al., 2023; Keawkumay et al., 2012; Nihmath & Ramesan, 2020; Nihmath & Ramesan, 2021).

The mechanical properties in terms of M100, M300, tensile strength, elongation at break, and hardness of NR and NR/VTES/RSi composites are summarized in Table 4.8. The M100 and M300 of NR and NR/VTES/RSi composites are displayed in Figure 4.12a. The addition of VTES/RSi to NR increased the M100 and M300 of NR because the filler with a higher stiffness than the matrix can increase the modulus of composite (Boonmahitthisud & Chuayjuljit, 2012; Bureewong et al., 2022a; Bureewong et al., 2022b). The M100 and M300 values of the composites are insignificant when RSi at the contents of 5 and 10 phr are added to NR. For the hardness properties, the addition of VTES/RSi to NR increased this property, which further increased with increasing VTES/RSi content, as shown in Figure 4.12d. This is because the stiffness of filler improves the resistance to indentation of NR. The tensile strength and elongation at break of NR and NR/VTES/RSi composites are displayed in Figures 4.12b and 4.12c, respectively. The addition of VTES/RSi to NR increased the tensile strength and elongation at break of NR, which indicates that the RSi combined with VTES can reinforce NR. Nevertheless, the increment of VTES/RSi content has no effect on the elongation at break of composites. In this study, the best condition is NR/2.0VTES/20RSi composite due to the result showing the highest value in the tensile strength.

Table 4.8 Mechanical properties of NR and NR/VTES/RSi composites.

Sample	M100 (MPa)	M300 (MPa)	Tensile strength (MPa)	Elongation at break (%)	Hardness (Shore A)
NR	0.65 ± 0.01	1.56 ± 0.03	7.18 ± 0.79	688.03 ± 34.27	26.70 ± 0.10
NR/0.5VTES/5RSi	0.86 ± 0.03	2.01 ± 0.05	14.76 ± 0.97	729.24 ± 29.23	35.00 ± 0.39
NR/1.0VTES/10RSi	0.85 ± 0.04	2.00 ± 0.10	14.16 ± 0.92	713.99 ± 20.66	36.00 ± 0.58
NR/2.0VTES/20RSi	1.14 ± 0.05	2.73 ± 0.16	18.94 ± 0.16	726.70 ± 17.74	40.90 ± 0.46

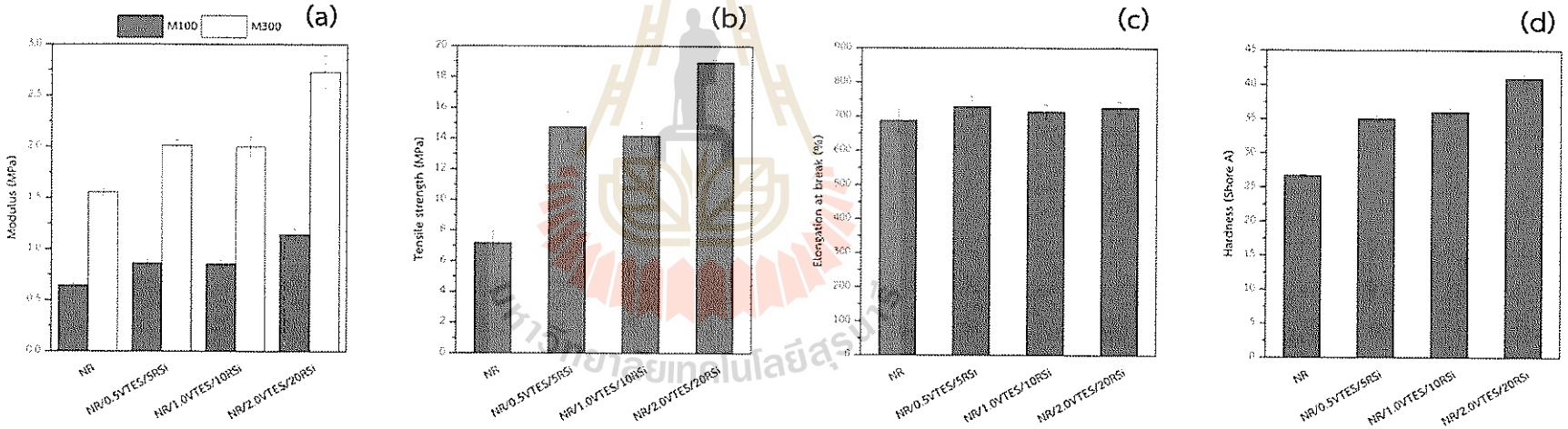

Figure 4.12 Mechanical properties of NR and NR/VTES/RSi composites showing (a) M100 and M300, (b) tensile strength, (c) elongation at break, and (d) hardness.

4.3.3 Morphological properties

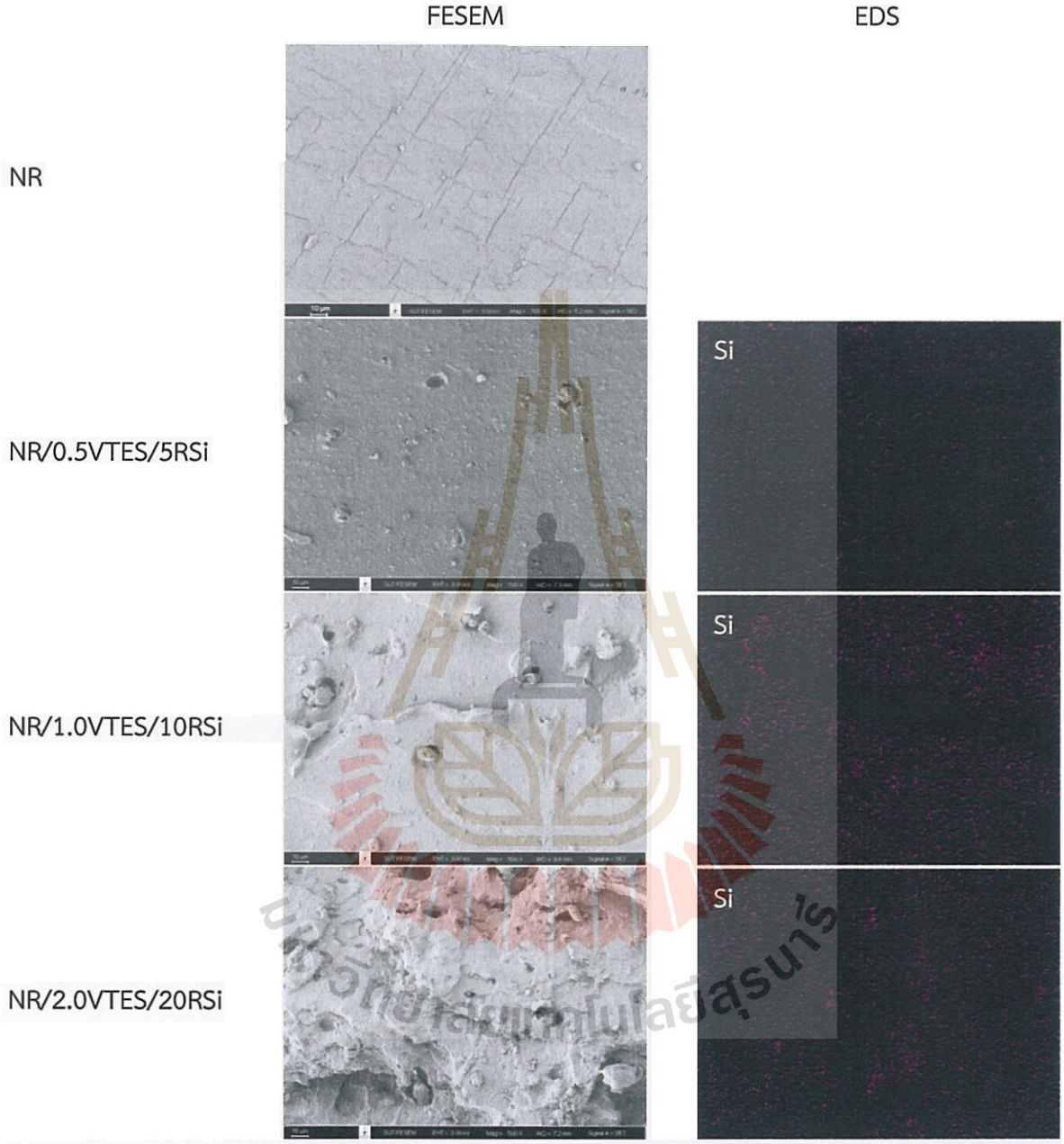

Figure 4.13 FESEM images and EDS mapping of fractured NR and NR/VTES/RSi composites.

The FESEM images and EDS mapping of fractured NR and NR/VTES/RSi composites are shown in Figure 4.13. The tensile fracture surface of NR shows a smooth surface without the Si element on the surface. On the other hand, the tensile fracture

surface of NR/VTES/RSi composite shows the dispersion and agglomeration of RSi particles on the surface. Where the agglomeration of RSi particles increased with increasing RSi content. This relates to the results of the EDS mapping of NR/VTES/RSi composites, which observed that the concentration and agglomeration of Si elements increased with increasing RSi content. Furthermore, the addition of VTES/RSi to NR increased the roughness of the tensile fracture surface of NR and further increased with increasing VTES/RSi content. The NR/VTES/RSi composite at the RSi contents of 5 and 10 phr show similarity in the size of RSi agglomeration on the tensile fracture surface. This relates to the fact that the mechanical properties of NR/VTES/RSi composites at these contents show insignificant values except for hardness properties.

4.4 Effect of RSi content on properties of NR/XSBR/RSi composites

Before the addition of RSi to NR/XSBR matrix. The NRL was blended with XSBRL at the ratios of 2:1, 1:1, and 1:2. Then drying, compounding, and vulcanizing to obtain the NR/XSBR blend. After that, the NR/XSBR blends were tested in terms of mechanical properties to find the optimal blending ratio of NR/XSBR.

The mechanical properties in terms of M100, M300, tensile strength, elongation at break, and hardness of NR, XSBR, and their blends are summarized in Table 4.9. The M100 and M300 of NR, XSBR, and their blends are displayed in Figure 4.14a. The blending of XSBR in NR increased the M100 and M300 of NR and further increased with increasing XSBR content. This is because the XSBR has a styrene component that is harder than NR, increasing the M100 and M300 of NR (Bureewong et al., 2022a; Tangudom et al.,, 2014). For the hardness properties, the blending of XSBR in NR showed the same trend as the M100 and M300, which are shown in Figure 4.14d. The tensile strength and elongation at break of NR, XSBR, and their blends are displayed in Figures 4.14b and 4.14c, respectively. The blending of XSBR in NR at a ratio of 2:1 showed the highest tensile strength and elongation at break of all the samples. This relates to the FESEM images of fractured NR, XSBR, and their blends, which are shown in Figure 4.15. The blending of XSBR in NR at a ratio of 2:1 revealed the roughness of the tensile fracture surface, indicating this blend is resistant to failure under tension (Stephen et al., 2003).

Table 4.9 Mechanical properties of NR, XSBR, and their blends.

Sample	M100 (MPa)	M300 (MPa)	Tensile strength (MPa)	Elongation at break (%)	Hardness (Shore A)
NR	0.65 ± 0.01	1.56 ± 0.03	7.18 ± 0.79	688.03 ± 34.27	26.70 ± 0.10
2NR/XSBR	0.78 ± 0.02	2.10 ± 0.04	14.63 ± 0.50	768.97 ± 13.34	26.77 ± 0.21
NR/XSBR	0.91 ± 0.01	2.83 ± 0.03	6.51 ± 0.45	466.99 ± 16.86	29.33 ± 0.15
NR/2XSBR	1.01 ± 0.05	3.20 ± 0.12	5.05 ± 0.90	388.46 ± 33.37	29.77 ± 0.64
XSBR	1.11 ± 0.04	3.45 ± 0.08	5.44 ± 0.23	389.23 ± 10.44	31.07 ± 0.15

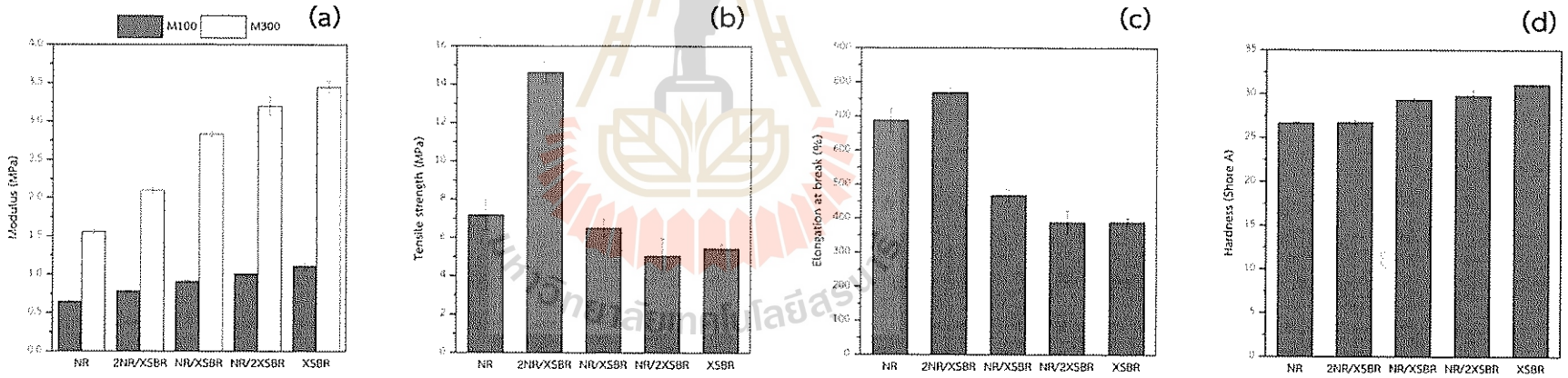

Figure 4.14 Mechanical properties of NR, XSBR, and their blends showing (a) M100 and M300, (b) tensile strength, (c) elongation at break, and (d) hardness.

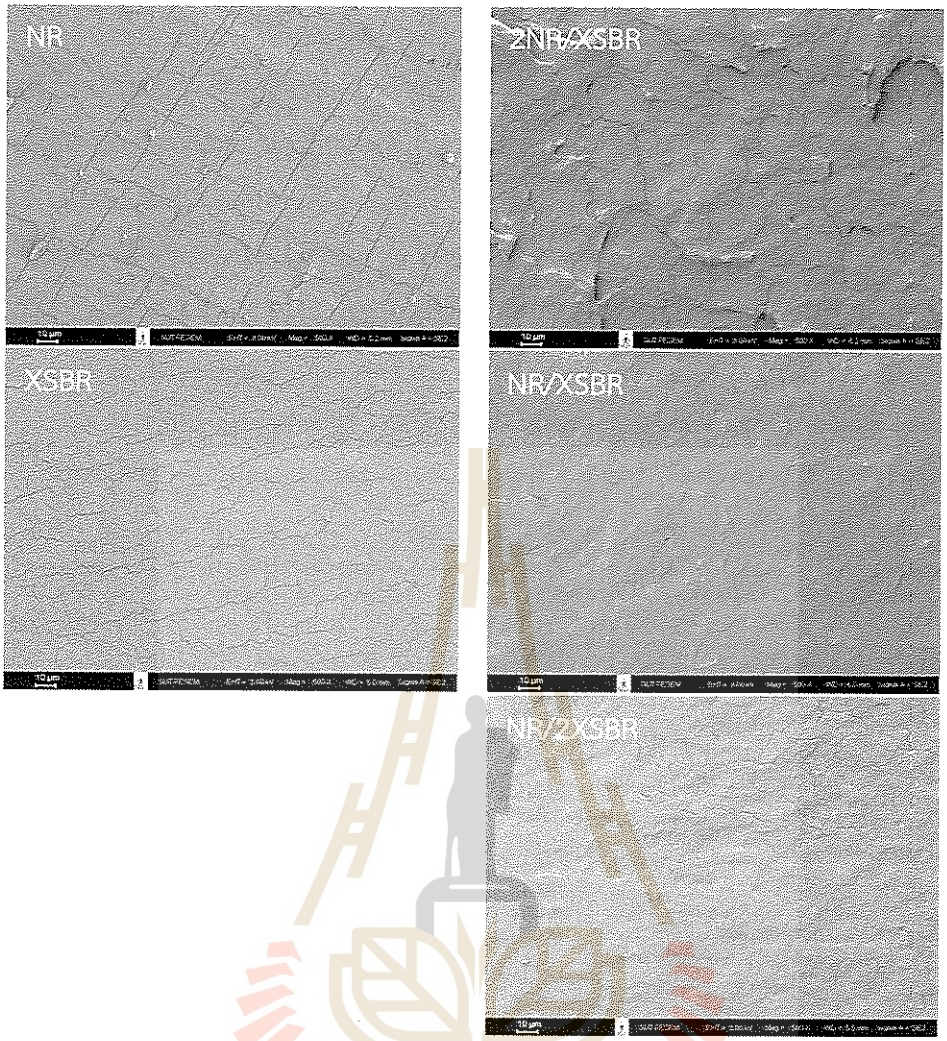

Figure 4.15 FESEM images of fractured NR, XSBR, and their blends.

4.4.1 Cure characteristics

The cure characteristics in terms of ML, MH, ts2, tc90, and cure rate index of 2NR/XSBR and 2NR/XSBR/RSi composites are summarized in Table 4.10. The ML and MH of 2NR/XSBR and 2NR/XSBR/RSi composites are displayed in Figure 4.16a. The addition of RSi to 2NR/XSBR tended to increase the MH of the blend because the stiffness of RSi increases the rigidity of composite vulcanizate. Nevertheless, the increment of RSi content exceeded 5 phr decreased the MH of the blend and further decreased with increasing RSi content. This is because the agglomeration of RSi particles in the blend, which is related to the FESEM images and EDS mapping of fractured 2NR/XSBR and 2NR/XSBR/RSi composites, which are shown in Figure 4.18 that revealed the RSi agglomeration in the 2NR/XSBR composite with RSi at the contents

of 10 and 20 phr. The ts2 and tc90 of 2NR/XSBR and 2NR/XSBR/RSi composites are displayed in Figure 4.16b. The addition of RSi to 2NR/XSBR decreased the ts2 and tc90 of the blend and further decreased with increasing RSi content. This is because the presence of sodium acetate generated from the RSi preparation acts as a catalyst and the increasing RSi content generates high heat from the filler attraction during the compounding, which enhances the vulcanization rate. As a result, the time required to vulcanize the rubber composites decreases (de Paiva et al., 2019; Phumnok et al., 2022). For the ML, the addition of RSi to 2NR/XSBR has no effect on this property.

Table 4.10 Cure characteristics of 2NR/XSBR and 2NR/XSBR/RSi composites.

Sample	ML (dNm)	MH (dNm)	ts2 (sec)	tc90 (sec)	Cure rate index (sec^{-1})
2NR/XSBR	9.17	17.36	123	544	0.24
2NR/XSBR/5RSi	9.50	22.32	93	200	0.93
2NR/XSBR/10RSi	9.87	20.04	87	173	1.16
2NR/XSBR/20RSi	9.72	17.43	53	143	1.11

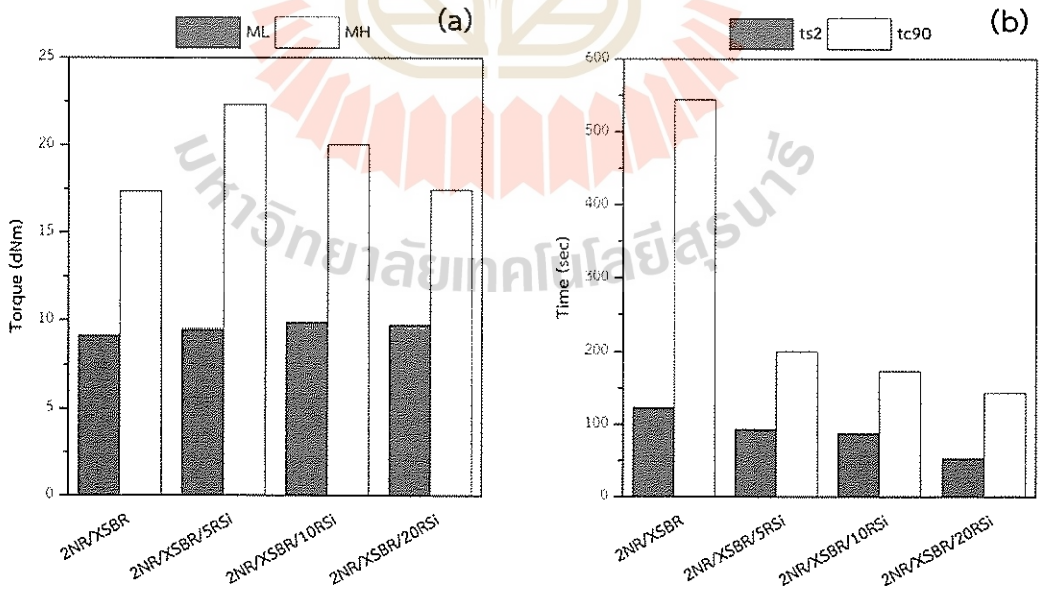

Figure 4.16 Cure characteristics of 2NR/XSBR and 2NR/XSBR/RSi composites showing (a) ML and MH and (b) ts2 and tc90.

4.4.2 Mechanical properties

The mechanical properties in terms of M100, M300, tensile strength, elongation at break, and hardness of 2NR/XSBR and 2NR/XSBR/RSi composites are summarized in Table 4.11. The M100 and M300 of 2NR/XSBR and 2NR/XSBR/RSi composites are displayed in Figure 4.17a. The addition of RSi to 2NR/XSBR increased the M100 and M300 of the blend and further increased with increasing RSi content because the filler with a higher stiffness than the matrix can increase the modulus of composite (Boonmahitthisud & Chuayjuljit, 2012; Bureewong et al., 2022a; Bureewong et al., 2022b). These properties show the same trend as the hardness properties of 2NR/XSBR and 2NR/XSBR/RSi composites, which are shown in Figure 4.17d. The tensile strength and elongation at break of 2NR/XSBR and 2NR/XSBR/RSi composites are displayed in Figures 4.17b and 4.17c, respectively. In this study, the addition of RSi to 2NR/XSBR at a content of 5 phr is the best condition because the addition of RSi at this content increases the tensile strength without affecting to the elongation at break of the blend. While the increment of RSi content exceeded 5 phr decreased the elongation at break of the blend and further decreased with increasing RSi content, especially the addition of RSi to 2NR/XSBR at a content of 20 phr also decreased the tensile strength of the blend. This relates to the FESEM images and EDS mapping of fractured 2NR/XSBR and 2NR/XSBR/RSi composites, which are shown in Figure 4.18. The addition of RSi to 2NR/XSBR at this content revealed the agglomeration of RSi particles in the large-size range on the blend surface, resulting in a drop in the tensile strength and elongation at break.

Table 4.11 Mechanical properties of 2NR/XSBR and 2NR/XSBR/RSi composites.

Sample	M100 (MPa)	M300 (MPa)	Tensile strength (MPa)	Elongation at break (%)	Hardness (Shore A)
2NR/XSBR	0.78 ± 0.02	2.10 ± 0.04	14.63 ± 0.50	768.97 ± 13.34	26.77 ± 0.21
2NR/XSBR/5RSi	0.95 ± 0.05	2.31 ± 0.11	15.46 ± 0.20	762.96 ± 23.71	33.37 ± 0.76
2NR/XSBR/10RSi	1.17 ± 0.06	2.81 ± 0.18	15.48 ± 0.35	725.71 ± 24.28	39.80 ± 0.26
2NR/XSBR/20RSi	1.54 ± 0.07	3.74 ± 0.24	12.29 ± 0.16	606.61 ± 22.81	46.57 ± 0.06

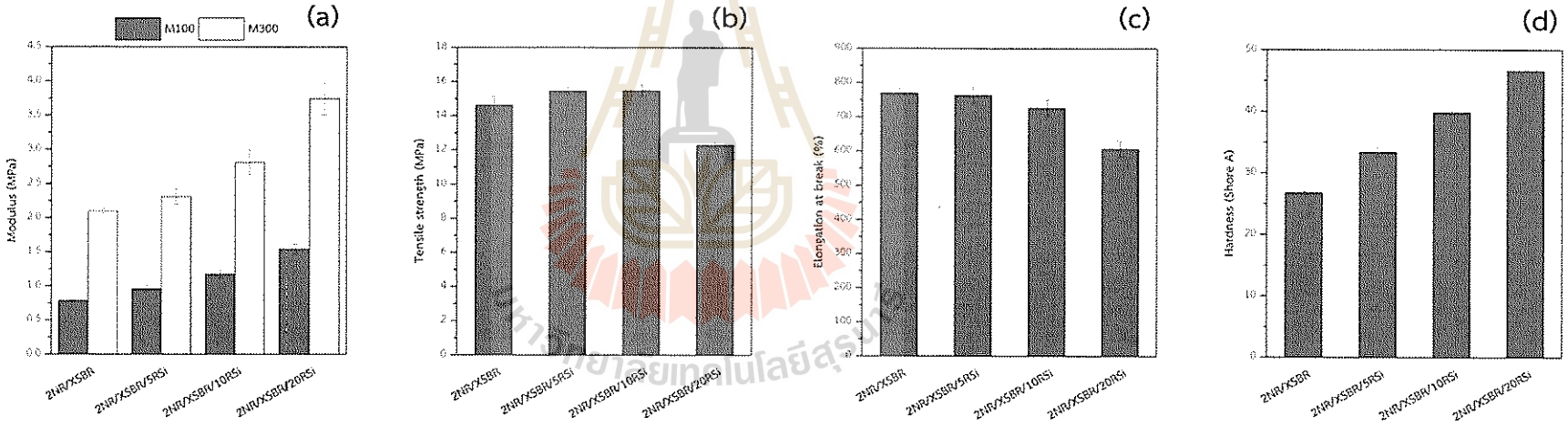

Figure 4.17 Mechanical properties of 2NR/XSBR and 2NR/XSBR/RSi composites showing (a) M100 and M300, (b) tensile strength, (c) elongation at break, and (d) hardness.

4.4.3 Morphological properties

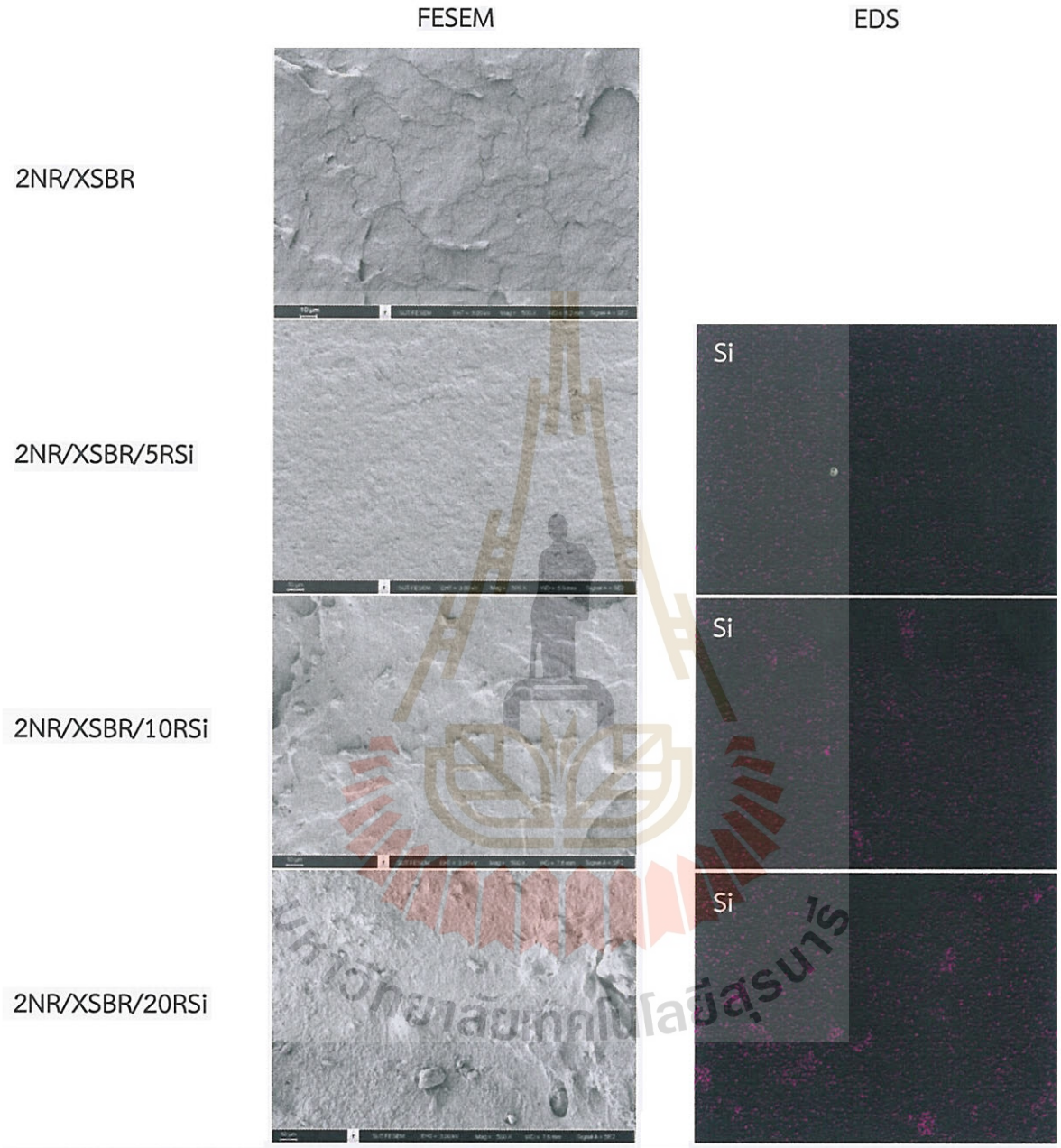

Figure 4.18 FESEM images and EDS mapping of fractured 2NR/XSBR and 2NR/XSBR/RSi composites.

The FESEM images and EDS mapping of fractured 2NR/XSBR and 2NR/XSBR/RSi composites are shown in Figure 4.18. The tensile fracture surface of 2NR/XSBR shows a roughness surface without the Si element on the surface. On the

other hand, the tensile fracture surface of 2NR/XSBR/RSi composite shows the dispersion and agglomeration of RSi particles on the surface. Where the agglomeration of RSi particles increased with increasing RSi content. This relates to the results of the EDS mapping of 2NR/XSBR/RSi composites, which observed that the concentration and agglomeration of Si elements increased with increasing RSi content. For the addition of RSi to 2NR/XSBR at a content of 20 phr, the FESEM image shows the agglomeration of RSi particles in the large-size range on the surface, resulting in a drop in the tensile strength and elongation at break of the blend. Thus, the RSi is an effective reinforcement filler until the size of RSi agglomeration is large.

4.5 Effect of polymer content on properties of PMM

Before the addition of polymer to cement. The mechanical properties in terms of tensile strength and elongation at break of NR/VTES/RSi and 2NR/XSBR/RSi composites were compared with those of NR and NR/RSi composites to find the optimal polymer composition.

The tensile strength and elongation at break of NR and rubber composites are summarized in Table 4.12. The use of VTES or XSBR to improve the functionality between NR and RSi can increase the tensile strength and elongation at break only at a RSi content of 5 phr. Then, the increment of RSi was greater than this content, decreasing the values of these properties. This is because the RSi agglomerates when these materials are added to the system, which reduces the efficiency of RSi reinforcement. However, the tensile strength and elongation at break of the use of VTES and XSBR with RSi at a content of 5 phr shows the values of these properties are almost equivalent to adding RSi at a content of 10 phr in NR. This may be an advantage as it can reduce the use of filler while maintaining good reinforcement efficiency. Where the use of XSBR with RSi at a content of 5 phr shows the higher of these properties than the use of VTES with RSi at the same content. Thus, the optimal polymer composition is 2NR/XSBR/5RSi composites, which are used as a polymer for further study of the addition content of polymer to cement.

Table 4.12 Mechanical properties of NR and rubber composites.

Sample	Tensile strength (MPa)	Elongation at break (%)
NR	7.18 ± 0.79	688.03 ± 34.27
NR/5RSi	12.34 ± 1.84	715.19 ± 9.16
NR/0.5VTES/5RSi	14.76 ± 0.97	729.24 ± 29.23
2NR/XSBR/5RSi	15.46 ± 0.20	762.96 ± 23.71
NR/10RSi	17.65 ± 1.42	730.56 ± 15.93
NR/1.0VTES/10RSi	14.16 ± 0.92	713.99 ± 20.66
2NR/XSBR/10RSi	15.48 ± 0.35	725.71 ± 24.28
NR/20RSi	20.86 ± 0.96	760.55 ± 53.63
NR/2.0VTES/20RSi	18.94 ± 0.16	726.70 ± 17.74
2NR/XSBR/20RSi	12.29 ± 0.16	606.61 ± 22.81

4.5.1 Mechanical properties

The mechanical properties in terms of tensile, flexural, and compressive strengths of unadded PMM and PMM are summarized in Table 4.13. The tensile strength of unadded PMM and PMM are displayed in Figure 4.19a.

Table 4.13 Mechanical properties of unadded PMM and PMM.

Sample	Tensile strength (MPa)	Flexural strength (MPa)	Compressive strength (MPa)
Unadded PMM	1.53 ± 0.09	5.47 ± 0.39	16.73 ± 1.91
0.05PMM	1.62 ± 0.01	3.77 ± 0.50	7.51 ± 0.50
0.10PMM	1.85 ± 0.28	4.24 ± 0.17	13.40 ± 0.30
0.20PMM	1.01 ± 0.17	2.17 ± 0.23	4.15 ± 0.54

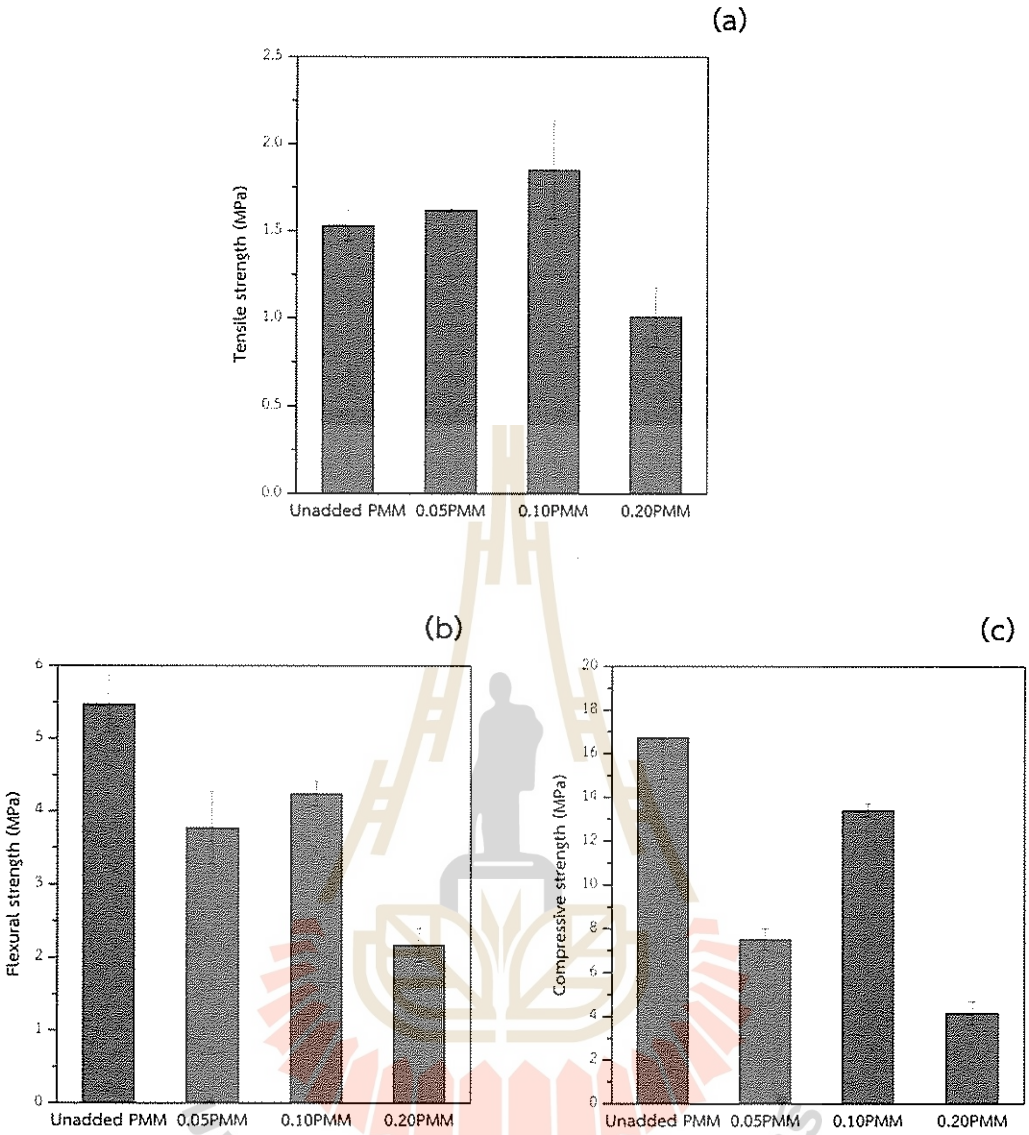

Figure 4.19 Mechanical properties of unadded PMM and PMM showing (a) tensile strength, (b) flexural strength, and (c) compressive strength.

The addition of polymer to cement increased the tensile strength and further increased with increasing polymer content. This is because the presence of polymer in the mortar that is coated on the surface and interconnected within the micropores of PMM can enhance the resistance in tension mode (Muhammad et al., 2011). However, the increment in a P/C ratio of 0.20 decreased this property of unadded PMM because the excess presence of polymer retards mortar packing and

generates more air pores in the structure. Figures 4.19b and 4.19c represent the flexural and compressive strengths of unadded PMM and PMM. The results of these properties show the same trend, which is that adding polymer to cement decreased these properties because of the retardation effect of polymer and voids from air bubbles (Sukmak et al., 2020). Thus, the addition of polymer to cement can improve the mechanical properties of unadded PMM only in the tensile strength. The P/C ratio of 0.10 is the optimal condition because it shows the highest tensile strength. Moreover, this condition also shows the highest flexural and compressive strengths when compared with the P/C ratios of 0.05 and 0.20.

4.5.2 Water absorption

The water absorption at different immersion times of 0.25, 1, 4, and 24 hours of unadded PMM and PMM are summarized in Table 4.14. All the samples showed an increase in the water absorption with increasing immersion time. Where a P/C ratio of 0.05 decreased the water absorption and further decreased with an increasing P/C ratio of 0.10. This is because the presence of polymer that is coated on the surface and interconnected within the micropores of PMM can block the water absorption that passes through the porosity of mortar. However, the increment in a P/C ratio of 0.20 increased the water absorption of unadded PMM because the excess presence of polymer retarded mortar packing and generated large air pores in the structure, creating a large room for absorption (Ismail et al., 2009).

Table 4.14 Water absorption of unadded PMM and PMM.

Sample	Water absorption (g/100 cm^2)			
	0.25 h	1 h	4 h	24 h
Unadded PMM	17.33 ± 2.31	36.00 ± 0.00	78.67 ± 2.31	102.67 ± 2.31
0.05PMM	9.33 ± 2.31	18.67 ± 2.31	34.67 ± 2.31	86.67 ± 6.11
0.10PMM	6.67 ± 2.31	14.67 ± 2.31	32.00 ± 4.00	76.00 ± 0.00
0.20PMM	48.00 ± 8.00	110.67 ± 6.11	133.33 ± 2.31	145.33 ± 4.62

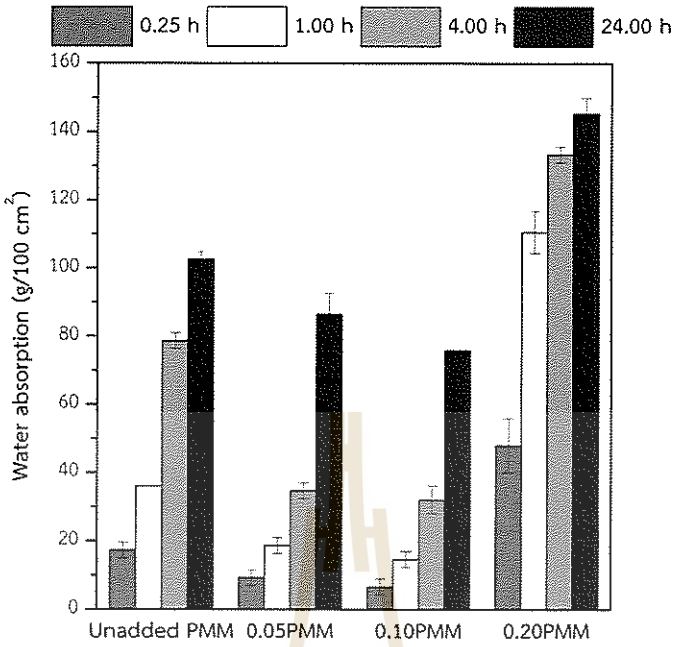

Figure 4.20 Water absorption at different immersion times of unadded PMM and PMM.

4.5.3 Morphological properties

The FESEM images of fractured surfaces of unadded PMM and PMM are shown in Figure 4.21. All the PMM images show the polymer films on the fractured surfaces, which show the polymer films stretching in some locations on the surfaces. Especially, the 0.20PMM that clearly observed the stretching of polymer films, which interconnected within the micropores of PMM. Additionally, it was found that the 0.20PMM has large air pores in the structure, which are the result of improper compaction of PMM. This is the reason for the decrease in mechanical properties and the increase in water absorption of 0.20PMM.

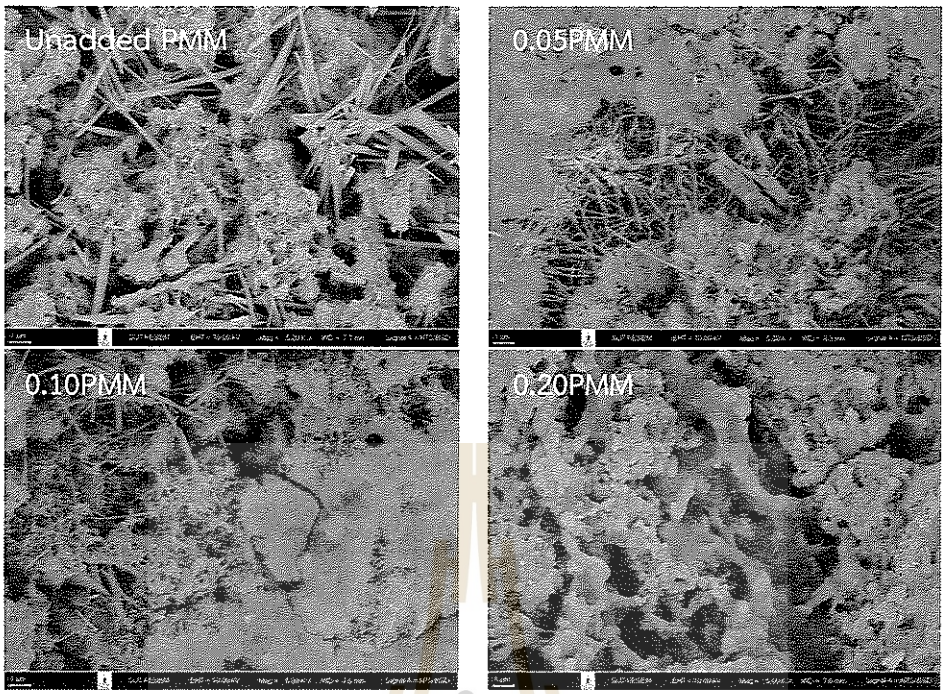

Figure 4.21 FESEM images of fractured surfaces of unadded PMM and PMM.

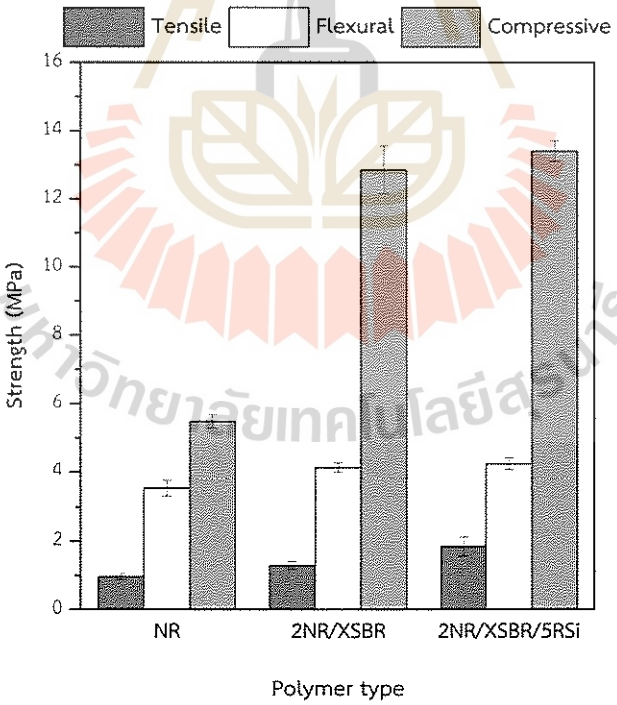

Figure 4.22 Mechanical properties of NR, 2NR/XSBR, and 2NR/XSBR/5RSi at the same content in mortar.

Confirming the presence of RSi and XSBR in polymer composition can improve the properties of PMM. The mechanical properties of NR, 2NR/XSBR, and 2NR/XSBR/5RSi at the same content in mortar were compared, as shown in Figure 4.22. For the results, the addition of 2NR/XSBR/5RSi in mortar showed the highest values in the tensile, flexural, and compressive strengths.

CHAPTER 5
CONCLUSION AND RECOMMENDATION

In this research, silica was prepared from RHA by the precipitation method and used as a filler in the rubber matrix. RSi had a purity of up to 99% and had a typical amorphous form. When comparing the RSi with CSi, it was found that RSi had a smaller particle size and a higher surface area than CSi.

Based on the mechanical properties of all rubber composites, it was found that the addition of RSi combined with VTES to NR and the addition of RSi to the blend showed higher tensile strength and elongation at break than RSi added to NR only at 5 phr. Where the addition of RSi to the blend showed higher tensile strength and elongation at break than the addition of RSi combined with VTES to NR. The addition of RSi to the blend at a content of 5 phr was used as a polymer for the study of the addition content of polymer to cement.

The polymer was added to cement at the polymer to cement (P/C) ratios of 0.00, 0.05, 0.10, and 0.20. The tensile strength of ordinary mortar increased with increasing P/C ratios until it reached a P/C ratio of 0.10. On the other hand, the flexural and compressive strengths of ordinary mortar decreased. When comparing the PMM at the P/C ratios of 0.05, 0.10, and 0.20, the PMM at a P/C ratio of 0.10 showed the highest values in flexural and compressive strengths. For the water absorption, the addition of polymer to cement reduced the water absorption of ordinary mortar with increasing P/C ratios until it reached a P/C ratio of 0.10.

According to the quality requirements for PMM in JIS A 6203, the polymer was added to cement at a P/C ratio of 0.10, showing the properties met the minimum requirements in the flexural and compressive strengths. For the water absorption, the 0.10PMM met this property only at 1 hour of immersion time. However, the use of this application still requires further research on several properties and practical use in the long-term.

REFERENCES

REFERENCES

Abdul Salim, Z. A. S., Hassan, A., & Ismail, H. (2018). A review on hybrid fillers in rubber composites. *Polymer-Plastics Technology and Engineering, 57*(6), 523-539.

Aggarwal, P., Singh, R. P., & Aggarwal, Y. (2015). Use of nano-silica in cement based materials—A review. *Cogent Engineering, 2*(1), 1078018.

Akbay, İ. K., Güngör, A., & Özdemir, T. (2018). Using fish scales (Sardina pilchardus) within ethylene ‐ propylene ‐ diene ter monomer rubber as bio ‐ based filler. *Journal of Applied Polymer Science, 135*(39), 46698.

Assaad, J. J. (2018). Development and use of polymer-modified cement for adhesive and repair applications. *Construction and Building Materials, 163*, 139-148.

Azat, S., Korobeinyk, A., Moustakas, K., & Inglezakis, V. (2019). Sustainable production of pure silica from rice husk waste in Kazakhstan. *Journal of cleaner production, 217*, 352-359.

Baghini, M. S., Ismail, A., Naseralavi, S. S., & Firoozi, A. A. (2016). Performance evaluation of road base stabilized with styrene–butadiene copolymer latex and Portland cement. *International Journal of Pavement Research and Technology, 9*(4), 321-336.

Balan, A. K., Mottakkunnu Parambil, S., Vakyath, S., Thulissery Velayudhan, J., Naduparambath, S., & Etathil, P. (2017). Coconut shell powder reinforced thermoplastic polyurethane/natural rubber blend-composites: effect of silane coupling agents on the mechanical and thermal properties of the composites. *Journal of materials science, 52*, 6712-6725.

Boonmahitthisud, A., & Chuayjuljit, S. (2012). NR/XSBR nanocomposites with carbon black and carbon nanotube prepared by latex compounding. *Journal of Metals, Materials and Minerals, 22*(1).

Boonmahitthisud, A., Pokphat, P., Chaiwutthinan, P., & Chuayjuljit, S. (2017). Nanocomposites of NR/SBR blend prepared by latex casting method: effects of nano-TiO2 and polystyrene-encapsulated nano-TiO2 on the cure characteristics, physical properties, and morphology. *Journal of Nanomaterials, 2017*.

Boonmee, A., & Jarukumjorn, K. (2020). Preparation and characterization of silica nanoparticles from sugarcane bagasse ash for using as a filler in natural rubber composites. *Polymer Bulletin, 77*(7), 3457-3472.

Bureewong, N., Injorhor, P., Krasaekun, S., Munchan, P., Waengdongbang, O., Wittayakun, J., . . . Ruksakulpiwat, Y. (2023). Preparation and Characterization of Acrylonitrile Butadiene Rubber Reinforced with Bio-Hydroxyapatite from Fish Scale. *Polymers, 15*(3), 729.

Bureewong, N., Ruksakulpiwat, Y., & Ruksakulpiwat, C. (2022a). IN SITU SILICA REINFORCED RUBBER LATEX COMPOSITE: EFFECTS OF BLEND RATIO AND SILICA CONTENT. *Suranaree Journal of Science & Technology, 29*(2).

Bureewong, N., Ruksakulpiwat, Y., & Ruksakulpiwat, C. (2022b). *Mechanical and thermal properties of NR/XSBR composite reinforced with rice husk silica.* Paper presented at the Journal of Physics: Conference Series.

Chuayjuljit, S., Nutchapong, T., Saravari, O., & Boonmahitthisud, A. (2015). Preparation and characterization of epoxidized natural rubber and epoxidized natural rubber/carboxylated styrene butadiene rubber blends. *Journal of Metals, Materials and Minerals, 25*(1).

de Paiva, F. F. G., de Maria, V. P. K., Torres, G. B., Dognani, G., dos Santos, R. J., Cabrera, F. C., & Job, A. E. (2019). Sugarcane bagasse fiber as semi-reinforcement filler in natural rubber composite sandals. *Journal of Material Cycles and Waste Management, 21*, 326-335.

Dhaneswara, D., Fatriansyah, J. F., Situmorang, F. W., & Haqoh, A. N. (2020). Synthesis of amorphous silica from rice husk ash: comparing HCl and CH3COOH acidification methods and various alkaline concentrations. *Synthesis, 11*(1), 200-208.

Dung, L. T. K., Hien, N. Q., Van Phu, D., & Du, B. D. (2017). Preparation and characterization of nanosilica from rice husk ash by chemical treatment combined with calcination. *Vietnam Journal of Chemistry, 55*(4), 455-455.

Guo, W., Li, G., Zheng, Y., & Li, K. (2021). Nano-silica extracted from rice husk and its application in acetic acid steam reforming. *RSC advances, 11*(55), 34915-34922.

Inphonlek, S., Bureewong, N., Jarukumjorn, K., Chumsamrong, P., Ruksakulpiwat, C., & Ruksakulpiwat, Y. (2022). Preparation of Poly (acrylic acid-co-acrylamide)-Grafted Deproteinized Natural Rubber and Its Effect on the Properties of Natural Rubber/Silica Composites. *Polymers, 14*(21), 4602.

Ismail, M., Muhammad, B., & Mohamad, N. A. (2009). Durability performance of natural rubber latex modified concrete. *Malaysian Journal of Civil Engineering, 21*(2).

Jembere, A. L., & Fanta, S. W. (2017). Studies on the synthesis of silica powder from rice husk ash as reinforcement filler in rubber tire tread part: Replacement of commercial precipitated silica. *SMR, 20*(70), 70.

Jo, B.-W., Kim, C.-H., Tae, G.-h., & Park, J.-B. (2007). Characteristics of cement mortar with nano-SiO2 particles. *Construction and Building Materials, 21*(6), 1351-1355.

Kato, H., Nakamura, A., & Noda, N. (2014). Determination of size distribution of silica nanoparticles: A comparison of scanning electron microscopy, dynamic light scattering, and flow field-flow fractionation with multiangle light scattering methods. *Materials Express, 4*(2), 144-152.

Keawkumay, C., Jarukumjorn, K., Wittayakun, J., & Suppakarn, N. (2012). Influences of surfactant content and type on physical properties of natural rubber/organoclay nanocomposites. *Journal of Polymer Research, 19*, 1-9.

Khan, K., Ullah, M. F., Shahzada, K., Amin, M. N., Bibi, T., Wahab, N., & Aljaafari, A. (2020). Effective use of micro-silica extracted from rice husk ash for the production of high-performance and sustainable cement mortar. *Construction and Building Materials, 258*, 119589.

Knapen, E., & Van Gemert, D. (2015). Polymer film formation in cement mortars modified with water-soluble polymers. *Cement and Concrete Composites, 58*, 23-28.

Kobler, J., Möller, K., & Bein, T. (2008). Colloidal suspensions of functionalized mesoporous silica nanoparticles. *Acs Nano, 2*(4), 791-799.

Loykaew, A., & Utara, S. (2020). Effect of acidic and sulfated environments on phase transformation, compressive strength and microstructure of natural rubber latex-modified cement pastes. *Journal of Materials Research and Technology, 9*(6), 15496-15512.

Majumder, C., Sharma, M., & Soni, G. (2014). A simple non-conventional method to extract amorphous silica from rice husk. *Bioresource Technology, accepted, 28*.

Muhammad, B., Ismail, M., Haron, Z., & Ali Yussuf, A. (2011). Elastomeric effect of natural rubber latex on compressive strength of concrete at high temperatures. *Journal of materials in civil engineering, 23*(12), 1697-1702.

Nawamawat, K., Sakdapipanich, J. T., Ho, C. C., Ma, Y., Song, J., & Vancso, J. G. (2011). Surface nanostructure of Hevea brasiliensis natural rubber latex particles. *Colloids and Surfaces A: Physicochemical and Engineering Aspects, 390*(1-3), 157-166.

Nihmath, A., & Ramesan, M. (2017). Fabrication, characterization and dielectric studies of NBR/hydroxyapatite nanocomposites. *Journal of Inorganic and Organometallic Polymers and Materials, 27*, 481-489.

Nihmath, A., & Ramesan, M. (2018). Preparation, characterization, thermal, and electrical properties of chlorinated ethylene propylene diene monomer/hydroxyapatite nanocomposites. *Polymer Composites, 39*(6), 2093-2100.

Nihmath, A., & Ramesan, M. (2020). Hydroxyapatite as a potential nanofiller in technologically useful chlorinated acrylonitrile butadiene rubber. *Polymer Testing, 91*, 106837.

Nihmath, A., & Ramesan, M. T. (2021). Development of hydroxyapatite nanoparticles reinforced chlorinated acrylonitrile butadiene rubber/chlorinated ethylene propylene diene monomer rubber blends. *Journal of Applied Polymer Science, 138*(15), 50189.

Ohama, Y., & Ramachandran, V. (1996). Polymer-modified mortars and concretes. In *Concrete admixtures handbook* (pp. 558-656): Elsevier.

Phumnok, E., Khongprom, P., & Ratanawilai, S. (2022). Preparation of natural rubber composites with high silica contents using a wet mixing process. *ACS omega, 7*(10), 8364-8376.

Pode, R. (2016). Potential applications of rice husk ash waste from rice husk biomass power plant. *Renewable and Sustainable Energy Reviews, 53*, 1468-1485.

Rabiei, S., & Shojaei, A. (2016). Vulcanization kinetics and reversion behavior of natural rubber/styrene-butadiene rubber blend filled with nanodiamond–The role of sulfur curing system. *European Polymer Journal, 81*, 98-113.

Rajan, V., Dierkes, W. K., Joseph, R., & Noordermeer, J. W. (2006). Science and technology of rubber reclamation with special attention to NR-based waste latex products. *Progress in Polymer Science, 31*(9), 811-834.

Rupasinghe, M., San Nicolas, R., Mendis, P., Sofi, M., & Ngo, T. (2017). Investigation of strength and hydration characteristics in nano-silica incorporated cement paste. *Cement and Concrete Composites, 80*, 17-30.

Shen, Y. (2017). Rice husk silica derived nanomaterials for sustainable applications. *Renewable and Sustainable Energy Reviews, 80*, 453-466.

Shen, Y., Zhao, P., & Shao, Q. (2014). Porous silica and carbon derived materials from rice husk pyrolysis char. *Microporous and Mesoporous Materials, 188*, 46-76.

Srisuwan, L., Jarukumjorn, K., & Suppakarn, N. (2018). Effect of silane treatment methods on physical properties of rice husk flour/natural rubber composites. *Advances in Materials Science and Engineering, 2018*.

Staudt, Y., Odenbreit, C., & Schneider, J. (2018). Failure behaviour of silicone adhesive in bonded connections with simple geometry. *International Journal of Adhesion and Adhesives, 82*, 126-138.

Stephen, R., Raju, K., Nair, S. V., Varghese, S., Oommen, Z., & Thomas, S. (2003). Mechanical and viscoelastic behavior of natural rubber and carboxylated styrene‐butadiene rubber latex blends. *Journal of Applied Polymer Science, 88*(11), 2639-2648.

Sukmak, G., Sukmak, P., Horpibulsuk, S., Yaowarat, T., Kunchariyakun, K., Patarapaiboolchai, O., & Arulrajah, A. (2020). Physical and mechanical properties of natural rubber modified cement paste. *Construction and Building Materials, 244*, 118319.

Tangudom, P., Thongsang, S., & Sombatsompop, N. (2014). Cure and mechanical properties and abrasive wear behavior of natural rubber, styrene–butadiene rubber and their blends reinforced with silica hybrid fillers. *Materials & Design, 53*, 856-864.

Thiele, G., Poston, M., & Brown, R. (2010). A case study in sizing nanoparticles. *Micromeritics Instrument Corporation. Available online: http://www. particletesting. com/library (accessed on 1 January 2019)*.

Thommes, M., Kaneko, K., Neimark, A. V., Olivier, J. P., Rodriguez-Reinoso, F., Rouquerol, J., & Sing, K. S. (2015). Physisorption of gases, with special reference to the evaluation of surface area and pore size distribution (IUPAC Technical Report). *Pure and applied chemistry, 87*(9-10), 1051-1069.

Thuadaij, N., & Nuntiya, A. (2008). Synthesis and characterization of nanosilica from rice husk ash prepared by precipitation method. *J. Nat. Sci. Special Issue on Nanotechnology, 7*(1), 59-65.

Vo, M. L., & Plank, J. (2018). Evaluation of natural rubber latex as film forming additive in cementitious mortar. *Construction and Building Materials, 169*, 93-99.

Vu, C. M., Vu, H. T., & Choi, H. J. (2015). Fabrication of natural rubber/epoxidized natural rubber/nanosilica nanocomposites and their physical characteristics. *Macromolecular Research, 23*, 284-290.

Wang, M., Wang, R., Yao, H., Farhan, S., Zheng, S., Wang, Z., . . . Jiang, H. (2016). Research on the mechanism of polymer latex modified cement. *Construction and Building Materials, 111*, 710-718.

Wang, R., Ma, D., Wang, P., & Wang, G. (2015). Study on waterproof mechanism of polymer-modified cement mortar. *Magazine of Concrete Research, 67*(18), 972-979.

Wei, Y., Zhang, H., Wu, L., Jin, L., & Liao, S. Q. (2017). *A review on characterization of molecular structure of natural rubber*.

Wongsorat, W., Suppakarn, N., & Jarukumjorn, K. (2014). Effects of compatibilizer type and fiber loading on mechanical properties and cure characteristics of sisal fiber/natural rubber composites. *Journal of Composite Materials, 48*(19), 2401-2411.

Yaowarat, T., Suddeepong, A., Hoy, M., Horpibulsuk, S., Takaikaew, T., Vichitcholchai, N., . . . Chinkulkijniwat, A. (2021). Improvement of flexural strength of concrete pavements using natural rubber latex. *Construction and Building Materials, 282*, 122704.

Yin, C., Zhang, Q., Liu, J., Gao, Y., Sun, Y., & Zhang, Q. (2019). Preparation and characterization of grafted natural rubber/graphene oxide nanocomposites. *Journal of Macromolecular Science, Part B, 58*(7), 645-658.

Yuvakkumar, R., Elango, V., Rajendran, V., & Kannan, N. (2014). High-purity nano silica powder from rice husk using a simple chemical method. *Journal of experimental nanoscience, 9*(3), 272-281.

Zhang, X., Du, M., Fang, H., Shi, M., Zhang, C., & Wang, F. (2021). Polymer-modified cement mortars: Their enhanced properties, applications, prospects, and challenges. *Construction and Building Materials, 299*, 124290.

APPENDIX A

SUPPLEMENTARY INFORMATION

SUPPLEMENTARY INFORMATION

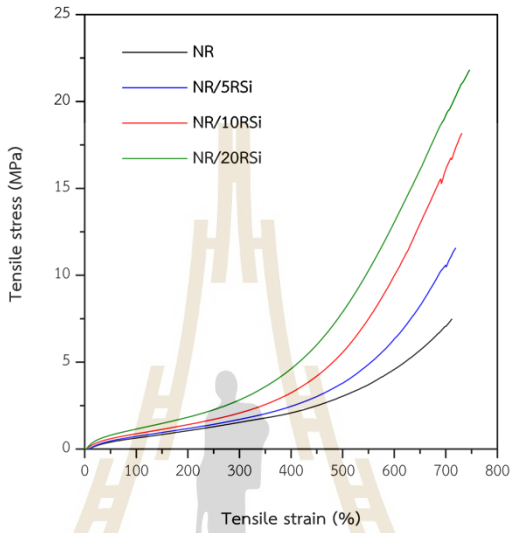

Figure A.1 Stress-strain curves of NR and NR/RSi composites.

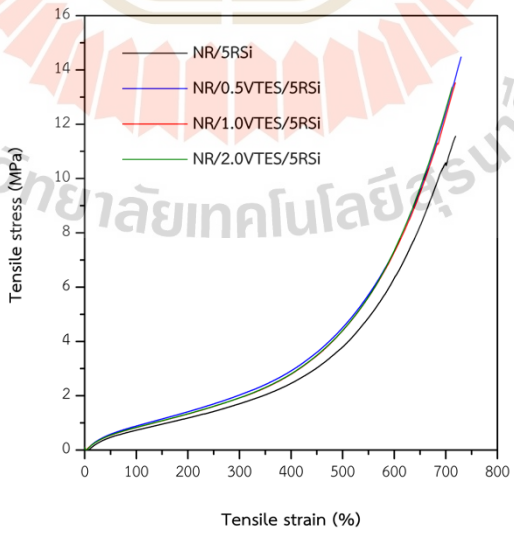

Figure A.2 Stress-strain curves of NR/5RSi and NR/VTES/5RSi composites.

SUPPLEMENTARY INFORMATION (Continued)

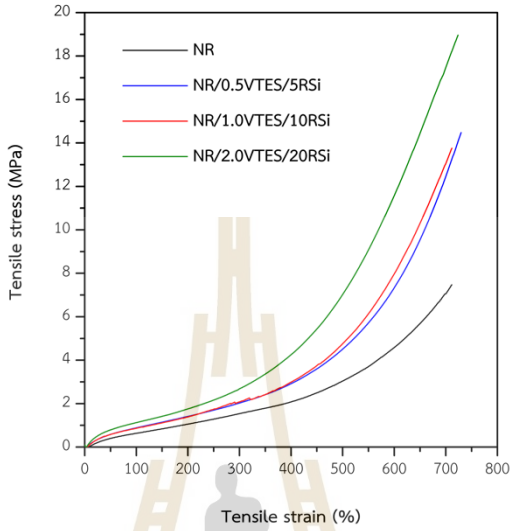

Figure A.3 Stress-strain curves of NR and NR/VTES/RSi composites.

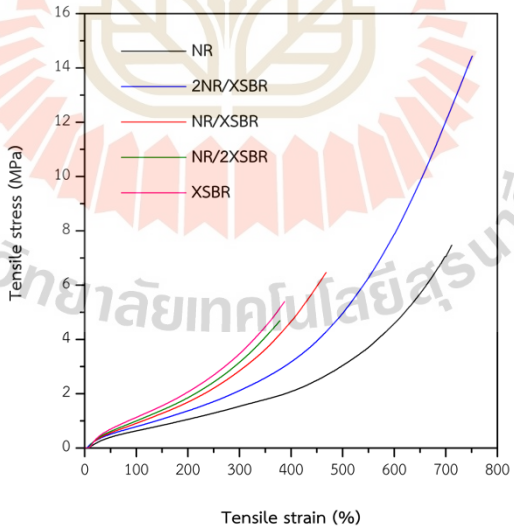

Figure A.4 Stress-strain curves of NR, XSBR, and their blends.

SUPPLEMENTARY INFORMATION (Continued)

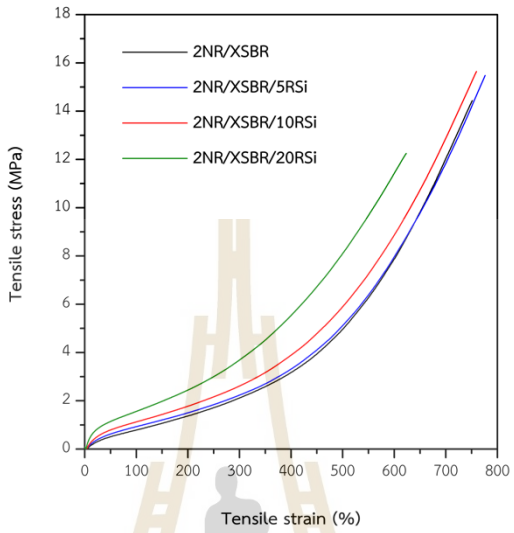

Figure A.5 Stress-strain curves of 2NR/XSBR and 2NR/XSBR/RSi composites.

Table A.1 Atomic percentages of unadded PMM and PMM.

Sample	Element (%)					
	C	O	Mg	Al	Si	Ca
Unadded PMM	15.71	64.83	0.24	1.04	3.72	14.47
0.05PMM	22.94	58.15	0.24	0.96	4.87	12.85
0.10PMM	23.87	54.16	0.66	1.20	6.31	13.81
0.20PMM	30.79	53.56	0.27	1.01	3.97	10.39

APPENDIX B

PUBLICATIONS

PUBLICATIONS

Bureewong, N., Ruksakulpiwat, Y., & Ruksakulpiwat, C. (2022a). IN SITU SILICA REINFORCED RUBBER LATEX COMPOSITE: EFFECTS OF BLEND RATIO AND SILICA CONTENT. *Suranaree Journal of Science & Technology, 29*(2).

Bureewong, N., Ruksakulpiwat, Y., & Ruksakulpiwat, C. (2022b). *Mechanical and thermal properties of NR/XSBR composite reinforced with rice husk silica.* Paper presented at the Journal of Physics: Conference Series.

IN SITU SILICA REINFORCED RUBBER LATEX COMPOSITE: EFFECTS OF BLEND RATIO AND SILICA CONTENT

Namthip Bureewong[1,2], Yupaporn Ruksakulpiwat[1,2] and Chaiwat Ruksakulpiwat[1,2,*]

Received: February 01, 2021; Revised: April 04, 2021; Accepted: April 04, 2021

Abstract

The effects of blend ratio and silica content were studied on mechanical, morphological, and thermal properties of rubber blends and composites. Natural rubber (NR) was blended with carboxylated styrene-butadiene rubber (XSBR) at different ratios of NR/XSBR, i.e., 1:1, 1:2, and 2:1. The optimum mechanical properties of NR/XSBR blends was obtained from NR/XSBR at the optimum ratio of 2:1. NR/XBSR with the optimum ratio was mixed with silica in silicate form. Commercial sodium silicate (CSS) was used to prepare the silica for use as reinforcing filler. NR/XSBR was firstly mixed with CSS to obtain the mixture of NR/XSBR/CSS. And then, acetic acid was dropped into the mixture to obtain the precipitated silica at various contents of silica (5, 10, and 20 phr). The addition of silica into NR/XSBR at the ratio of 2:1 can improve the thermal property of the NR/XSBR blends. By increasing silica contents, an insignificant difference in terms of tensile strength and elongation at break of the mechanical properties was observed. The best thermal properties were obtained from NR/XSBR/20Si composite.

Keywords: **Natural rubber latex, Carboxylated styrene-butadiene rubber latex, Rubber blend, Silica, Rubber composite**

Introduction

Natural rubber (NR) is one of the important agricultural products of Thailand that can be used to produce a wide of products due to high resilience, good tensile strength, and tear resistance, etc. (Chuayjuljit *et al*., 2015; Vu *et al*., 2015). The making of NR products covered many industries such as automotive (tires, belts, and seals), medical (gloves, tubes, and condoms), and others (shoes, furniture, and sponges), etc. (Rajan *et al*., 2006). However, NR is known that has low resistance for sunlight, ozone, and oxygen or heat aging because it contains the double bonds in the molecular structure (Jones and Tinker, 1997; Vu *et al*., 2015). Therefore, the most productive of NR production are not preferred to use only NR but will be used with other rubbers or fillers to obtain the properties of the product required (Varkey *et al*., 2000; Motaung *et al*., 2011). The samples of manufacturing of tires

[1] *School of Polymer Engineering, Institute of Engineering, Suranaree University of Technology, Nakhon Ratchasima, 30000, Thailand. Tel. 0-4422-3613, Fax. 0-4422-4605, E-mail: Charuk@sut.ac.th*
[2] *Center of Excellence on Petrochemical and Materials Technology, Chulalongkorn University, Bangkok, 10330, Thailand.*
[*] *Corresponding author*

were applied for NR with butadiene rubber (BR) or styrene-butadiene rubber (SBR), carbon black, and silica for improving wear, traction, and rolling resistance, etc. (Le *et al*., 2010; Shan *et al*., 2011).

The other rubbers and fillers, SBR and silica are interesting because they can improve some properties of NR such as mechanical and thermal properties. Varkey *et al*. (2000) studied the thermal degradation of NR/SBR latex blends by using the thermogravimetric method and they found that blending with SBR increased the thermal stability of NR. Poompradub *et al*. (2014) reported that the filling NR with in situ silica can not improve only the mechanical properties but also the thermal properties of the filled vulcanizates, and was superior compared with the ex-situ silica. SBR is the largest volume of synthetic rubber. It can polymerize by using the solution or emulsion technique. Moreover, it has the low reversion of resistance, high resistance of abrasion at higher speeds, and good resistance for flexible fatigue. However, the main drawbacks of SBR are poor oil and ozone resistances. The carboxylated SBR (XSBR) is one of the members of SBR polymerized with the emulsion polymerization of styrene, butadiene, and some strong acid monomer that like acrylic acid or methyl methacrylate acid. It has the good abrasion resistance, aging stability, hydrocarbon solvent resistance, and interaction with the functional filler that like silica (Alimardani and Abbassi-sourki, 2014). There are several reports that mentioned about the NR blended with XSBR to easily modify the mechanical properties of NR because of the polarity of XSBR (Stephen *et al*., 2003). Also, the incorporation of XSBR into NR improves the thermal properties and gas permeability of NR (Stephen *et al*., 2005). Silica is the important filler in the rubber industry that reduces heat buildup and improves the tensile strength, tear strength, and abrasion resistance of rubber composites (Ikeda and Kohjiya, 1997; Kohjiya and Ikeda, 2003). Moreover, it is known that in the tire industry, silica is extensively used to substitute with carbon black for reducing the rolling resistance of tire treads and enhance wet grip (Alimardani and Abbassi-sourki, 2014). Nevertheless, the above reports generally mentioned the mixing of rubber in a latex form which compounding of latex is the low energy of processing of consumption but normal interaction between filler and rubber that not good because there is not present the mastication step (Stephen *et al*., 2006). Therefore, using of XSBR blended with NR composites may be solved this problem because it contained carboxyl groups which may be reduced the mastication step and compatible with silica that used as the filler in this study.

The aim of this research is focused on study of the effects of blend ratio between NR and XSBR at the ratio of 1:1, 1:2, and 2:1 on the mechanical, morphological, and thermal properties. The optimum NR/XSBR ratio was mixed with in situ silica at various contents (5, 10, and 20 phr). Mechanical, morphological, and thermal properties of NR/XSBR/Si composites were studied.

Materials and Methods

Materials

Natural rubber latex (NRL) with a solids content of 60wt% and high ammonia-treated latex was supplied by Chemical & Materials Co., Ltd. Carboxylated styrene-butadiene rubber latex (XSBRL) was supplied by Jorakay Corporation Co., Ltd. Commercial sodium silicate (CSS) was supplied by Sigma-Aldrich Co., Ltd. Acetic acid was supplied by Merck & Co., Inc. Zinc oxide (ZnO), stearic acid, N-Cyclohexyl-2-Benzothiazole Sulfonamide (CBS), and sulfur were supported by Chemical Innovation Co., Ltd.

Preparation of NR/XSBR Sheets

NRL was blended with XSBRL at different ratios of NR/XSBR, i.e., 1:1, 1:2, and 2:1 by using a magnetic stirrer for 30 mins. Rubber mixtures were poured onto the Teflon tray and dried at 60°C by using a hot air oven for 16 hr to obtain NR/XSBR sheets.

Preparation of NR/XSBR/Si Sheets

NR/XSBR at the ratio of 2:1 was mixed with CSS at various contents of silica (5, 10 and 20 phr) by using a magnetic stirrer for 30 mins to obtain NR/XSBR/CSS mixtures. Acetic acid was dropped into the NR/XSBR/CSS mixture until neutral to gain precipitated silica. The mixtures were poured onto the Teflon tray and dried at 60°C by using a hot air oven for 16 h to obtain NR/XSBR/Si sheets.

Preparation of NR/XSBR Blends and NR/XSBR/Si Composites

All samples were mixed with 5 phr ZnO, 2 phr stearic acid, 2.5 phr CBS, and 1 phr sulfur by using a two-roll mill machine to obtain compounds. Vulcanization of all compounds was done by using the compression molding machine at 150°C with optimum curing time (t_c90) that determined by Moving Die Rheometer (MDR) to obtain NR/XSBR blends and NR/XSBR/Si composites.

Mechanical Properties

The tensile properties of blends and composites were measured according to ASTM

D412 using a Universal Testing Machine (Instron 5565) with a crosshead speed of 500 mm/min and a load cell of 5 kN.

The hardness of blends and composites were measured according to ASTM D2240 using a Bareiss shore A (HPE II).

Morphological Properties

The morphology of blends and composites were investigated by Field Emission Scanning Electron Microscope (FE-SEM) using a Carl Zeiss (Auriga). All of the samples were coated with gold before testing.

Thermal Properties

The thermal stability of blends and composites were determined by thermogravimetric analysis (TGA) using a Mettler Toledo (TGA/DSC1). All samples were placed into an alumina pan and heated at the room temperature up to 800°C under nitrogen at a heating rate of 10°C /min.

Results and Discussion

Mechanical Properties of NR/XSBR Blends

The mechanical properties of NR, XSBR, and NR/XSBR at different ratios of blending are shown in Figure 1. All NR/XSBR blends showed higher modulus at 100% and 300% elongation than NR but lower than XSBR depending on the ratios of blending. This is because XSBR has a styrene content for making the XSBR harder and rubbery less than NR. NR/XSBR at the ratio of 2:1 showed the highest tensile strength and elongation at break due to its strain-induced crystallization (Stephen *et al*., 2003). However, all NR/XSBR blends showed an insignificant difference of hardness.

Morphological Properties of NR/XSBR Blends

The morphological properties of NR, XSBR, and NR/XSBR at different ratios of blending are shown in Figure 2. The surface fracture by using the tensile testing of XSBR showed the flattest surface when compared with NR and NR/XSBR at different ratios of blending. The surface roughness of NR/XSBR increased with NR content. The highest surface roughness was obtained from NR/XSBR at the ratio of 2:1. The rough fractured surface indicate that the samples was failed in a ductile manner which led to the good elongation at break (Boonmahitthisud *et al*., 2017).

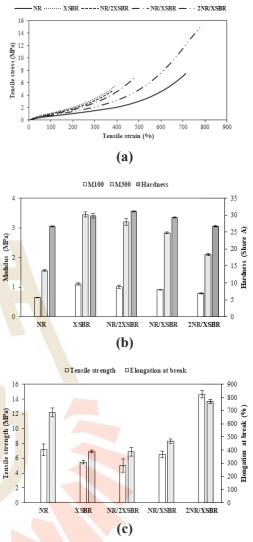

Figure 1. Mechanical properties of NR, XSBR, and NR/XSBR blends showing (a) stress-strain curve, (b) modulus at 100% elongation, modulus at 300% elongation, and hardness, and (c) tensile strength and elongation at break.

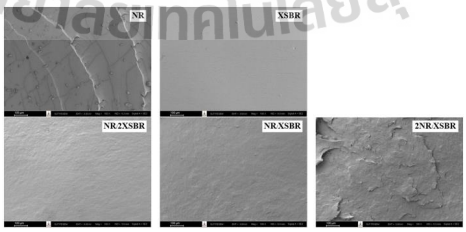

Figure 2. SEM images of NR, XSBR, and NR/XSBR blends.

Table 1. Degradation temperature at different weight loss levels of NR, XSBR, NR/XSBR blends, NR/XSBR/Si composites, and silica.

Sample	$T_{30\%}$ (°C)	$T_{50\%}$ (°C)	$T_{70\%}$ (°C)	T_{max} (°C)
NR/XSBR Blends				
NR	366	380	397	378
XSBR	401	421	442	415
2NR/XSBR	371	390	415	388
NR/XSBR/Si Composites				
2NR/XSBR/5Si	373	392	421	389
2NR/XSBR/10Si	376	400	433	390
2NR/XSBR/20Si	371	397	434	389
Silica	449	N/A	N/A	483

Thermal Properties of NR/XSBR Blends

The thermal properties in term of degradation of temperature at different levels of weight loss of NR, XSBR, and NR/XSBR at the ratios of 2:1 are listed in Table 1. NR showed the lowest degradation temperature compared with XSBR and NR/XSBR at the ratio of 2:1 because NR is a diene rubber that is highly susceptibility to degrade (Stephen *et al*., 2006). NR/XSBR at the ratio of 2:1 showed higher degradation temperature than NR while XSBR showed the highest degradation temperature. XSBR can increase the degradation temperature of the NR/XSBR blend.

Mechanical Properties of NR/ XSBR/ Si Composites

NR/XSBR at the ratio of 2:1 was selected to be blended with silica at the different contents.

The mechanical properties of NR/XSBR and NR/XSBR blended with silica at different contents are shown in Figure 3. The modulus at 100% and 300% elongation of all NR/XSBR blended with silica were higher than those of NR/XSBR blends. With increasing silica contents, modulus at 100% and 300% elongation were higher due to the higher stiffness of fillers. That is the reason of the results of the hardness of NR/XSBR and NR/XSBR blended with silica at the different contents as well. However, NR/XSBR and NR/XSBR blended with silica at different contents showed a slight difference in tensile strength and elongation at break.

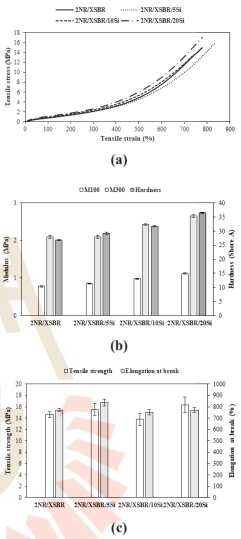

Figure 3. Mechanical properties of NR/XSBR blend and NR/XSBR/Si composites showing (a) stress-strain curve, (b) modulus at 100% elongation, modulus at 300% elongation, and hardness, and (c) tensile strength and elongation at break.

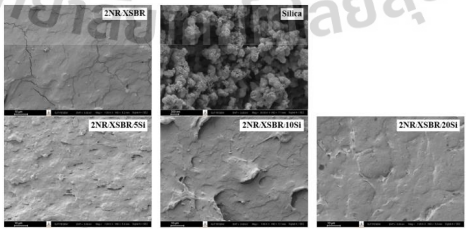

Figure 4. SEM images of NR/XSBR blend, silica, and NR/XSBR/Si composites.

Morphological Properties of NR/XSBR/Si Composites

The morphological properties of silica, NR/XSBR, and NR/XSBR blended with silica at different contents are shown in Figure 4. The surface fracture obtained from tensile testing of NR/XSBR showed a slightly rough surface when compared with NR/XSBR blended with silica at different contents. All NR/XSBR blended with silica showed similar rough surfaces. This led to the slight difference in elongation at break of NR/XSBR and NR/XSBR blended with silica at different contents since fracture surface can indicate failure manner which affected to the mechanical properties of samples. Silica particles were prepared by dropping acetic acid in CSS until neutral. This showed silica particles in a general form that is in spherical structure and partially agglomerated due to filler- filler interactions of silica (Choi, 2001; Stephen *et al*., 2007).

Thermal Properties of NR/XSBR/Si Composites

The thermal properties in term of degradation temperature of NR/ XSBR and NR/ XSBR blended with silica at different contents are listed in Table 1. The degradation temperature of NR/XSBR and NR/XSBR blended with silica at the different contents showed an insignificant difference in degradation temperature in the early weight loss levels of degradation. However, considering 70% weight loss level it was found that the degradation temperature of NR/XSBR/Si composites increased with the addition of silica, due to the higher thermal stability of silica than NR and XSBR.

Conclusions

The blending of NR and XSBR can improve the thermal properties of NR. NR/ XSBR at the ratio of 2:1 showed the highest tensile strength about 200% when compared with NR. The addition of silica into NR/XSBR at the ratio of 2:1 can improve the thermal properties of NR/XSBR blends with an insignificant difference in mechanical properties in terms of tensile strength and elongation at break. NR/XSBR at the ratio of 2:1 showed an increase in degradation temperature with increasing silica contents. Therefore, the best thermal properties were obtained from NR/XSBR/20Si composite.

Acknowledgments

The authors are grateful for financial supports from the Center of Excellence on Petrochemical and Materials Technology (PETROMAT) and chemicals for rubber compounding from the Chemical Innovation Co., Ltd.

References

Alimardani, Mohammad and Foroud Abbassi-sourki. (2014). New and emerging applications of carboxylated styrene butadiene rubber latex in polymer composites and blends: Review from structure to future prospective. J. Composite Materials., 49.

Boonmahitthisud, Anyaporn., Peeraphong Pokphat., Phasawat Chaiwutthinan., and Saowaroj Chuayjuljit. (2017). Nanocomposites of NR/SBR blend prepared by latex casting method: effects of nano-TiO2 and polystyrene-encapsulated nano-TiO2 on the cure characteristics, physical properties, and morphology. J. Nanomaterials., 2017.

Choi, Sung-Seen. (2001). Improvement of properties of silica-filled styrene-butadiene rubber compounds using acrylonitrile-butadiene rubber. J. applied polymer scien., 79:1127-33.

Chuayjuljit, Saowaroj., Thongchai Nutchapong., Onusa Saravari., and Anyaporn Boonmahitthisud. (2015). Preparation and characterization of epoxidized natural rubber and epoxidized natural rubber/carboxylated styrene butadiene rubber blends. J. Metals, Materials and Minerals., 25.

Ikeda, Yuko and Shinzo Kohjiya. (1997). In situ formed silica particles in rubber vulcanizate by the sol-gel method. Polymer, 38; 4417-23.

Jones, KC and Andrew Tinker. (1997). Blends of natural rubber: Novel techniques for blending with specialty polymers (Springer Science & Business Media).

Kohjiya, S and Y Ikeda. (2003). In situ formation of particulate silica in natural rubber matrix by the sol-gel reaction. J. sol-gel scien. and technol., 26:495-98.

Le, Hai Hong., Sybill Ilisch., Daniel Heidenreich., André Wutzler, and Hans-Joachim Radusch. (2010). Kinetics of the phase selective localization of silica in rubber blends. Polymer composites., 31:1701-11.

Motaung, Tshwafo E., Adriaan S Luyt., and Sabu Thomas. (2011). Morphology and properties of NR/EPDM rubber blends filled with small amounts of titania nanoparticles. Polymer composites., 32:1289-96.

Poompradub, Sirilux., Mantana Thirakulrati., and Pattarapan Prasassarakich. (2014). In situ generated silica in natural rubber latex via the sol-gel technique and properties of the silica rubber composites. Materials Chem. and Phy., 144:122-31.

Rajan, VV., Wilma K Dierkes., R Joseph., and Jacobus WM Noordermeer. (2006). Science and technology of rubber reclamation with special attention to NR-based waste latex products. Progress in polymer scien., 31:811-34.

Shan, Chunpeng., Zheng Gu., Li Wang., Peiyao Li., Guojun Song., Zhenbin Gao., and Xiaoyu Yang. (2011). Preparation, characterization, and application of NR/SBR/Organoclay nanocomposites in the tire industry. J. applied polymer scien., 119:1185-94.

Stephen, Ranimol., AM Siddique., Fouran Singh., Lekshmi Kailas., Seno Jose., Kuruvilla Joseph., and Sabu Thomas. (2007). Thermal degradation and ageing behavior of microcomposites of natural rubber, carboxylated styrene butadiene rubber latices, and their blends. J. applied polymer scien., 105:341-51.

Stephen, Ranimol., KVSN Raju., Sobha V Nair., Siby Varghese., Zachariah Oommen., and Sabu Thomas. (2003). Mechanical and viscoelastic behavior of natural rubber

and carboxylated styrene-butadiene rubber latex blends. J. applied polymer scien., 88:2639-48.

Stephen, Ranimol., Sabu Thomas., and Kuruvilla Joseph. (2005). Gas permeation studies of natural rubber and carboxylated styrene-butadiene rubber latex membranes. J. applied polymer scien., 98:1,125-34.

Stephen, Ranimol., Seno Jose., Kuruvilla Joseph., Sabu Thomas., and Zachariah Oommen. (2006). Thermal stability and ageing properties of sulphur and gamma radiation vulcanized natural rubber (NR) and carboxylated styrene butadiene rubber (XSBR) latices and their blends. Polymer Degradation and Stability., 91:1717-25.

Varkey, Jyothi T., Sunny Augustine., and Sabu Thomas. (2000). Thermal degradation of natural rubber/styrene butadiene rubber latex blends by thermogravimetric method. Polymer-Plastics Technol. and Eng., 39:415-35.

Vu, Cuong Manh., Huong Thi Vu., and Hyoung Jin Choi. (2015). Fabrication of natural rubber/epoxidized natural rubber/nanosilica nanocomposites and their physical characteristics. Macromolecular Research., 23:284-90.

IUMRS-ICA 2021 IOP Publishing
Journal of Physics: Conference Series **2175** (2022) 012017 doi:10.1088/1742-6596/2175/1/012017

Mechanical and thermal properties of NR/XSBR composite reinforced with rice husk silica

Namthip Bureewong[1,2], Yupaporn Ruksakulpiwat[1,2], Chaiwat Ruksakulpiwat[1,2]

[1] School of Polymer Engineering, Institution of Engineering, Suranaree University of Technology, Nakhon Ratchasima 30000, Thailand.
[2] Center of Excellence on Petrochemical and Materials Technology, Chulalongkorn University, Bangkok 10330, Thailand.

E-mail: Charuk@sut.ac.th

Abstract. Natural rubber (NR) is a renewable resource that is used in many products. In the production of NR products, other rubbers or fillers may be used to produce a product with required properties. However, most rubbers and fillers are synthetic which are non-environmentally friendly materials. To solve this problem, rice husk ash (RHA) from biomass power plant was used to prepare silica to be used as a filler in rubber by in-situ generation. The purer RHA was prepared by leaching with HCl to remove some metallics and increase silica contents by combustion. The purer RHA was dissolved in NaOH to obtain sodium silicate from RHA (RSS). Carboxylated styrene-butadiene rubber (XSBR) used as synthetic rubber was blended with NR in latex form. NR/XSBR at the ratio of 2:1 was mixed with RSS to obtain NR/XSBR/RSS mixture. Acetic acid was dropped into the mixture until neutral for precipitating silica to obtain NR/XSBR/RSi composite. The mechanical, morphological, and thermal properties of NR/XSBR/RSi composites at different contents of silica (5, 10, and 15 phr) were studied. The NR/XSBR/RSi composite with optimum content was compared with NR/XSBR/CSi composite which prepared silica from commercial sodium silicate (CSS) on mechanical, morphological, and thermal properties.

Keywords: Natural rubber latex, Carboxylated styrene-butadiene rubber latex, Rice husk ash, Silica, Rubber composite

1. Introduction

Natural rubber (NR) is one of Thailand's important renewable resource which can be used to produce in many products because it has high resilience, good tensile strength, tear resistance, etc. (1, 2). This is the reason of NR products covering in many industries such as automotive, medical, construction, etc. (3).

However, it is known that NR has low resistance to sunlight, ozone, and oxygen or heat aging because it consists of double bonds in the molecular structure (4). Therefore, the production of most NR products is not used only NR but also used it with other rubbers or fillers to obtain the required product properties (5, 6). For example, the tire manufacturers used NR with butadiene rubber (BR) or

styrene-butadiene rubber (SBR), carbon black (CB), and silica to improve wear, traction, rolling resistance, etc. (7, 8).

In the other rubbers and fillers, carboxylated SBR (XSBR) and silica are interesting materials because they can improve some NR properties such as mechanical and thermal properties. There are several reports mentioned that NR blended with XSBR which can easily modify the mechanical properties of NR and the incorporation of XSBR into NR can improve the thermal properties and gas permeability of NR (9). Poompradub et al. reported that filling NR with in-situ silica can improve not only the mechanical properties but also the thermal properties and it is superior compared with using ex-situ silica (10). However, it is known that these are synthetic that are non-environmentally friendly materials. Therefore, this research is to study in reducing this problem by using rice husk ash (RHA) from biomass power plant to prepare silica used as a filler in rubber by in-situ generation.

RHA is one of agricultural wastes that consists of high silica content in amorphous form that can be used in many applications such as adsorbent, catalyst, fertilizer, etc. (11). In-situ silica has several advantages, including enhanced silica dispersion, higher silica loading in the matrix, possible to customize the particle size, and energy-efficient processing (12).

This research aims to study the effect of rice husk silica (RSi) contents in NR/XSBR blend on mechanical, morphological, and thermal properties. The effect of silica sources was also studied by comparison between NR/XSBR/RSi composite with NR/XSBR/CSi composite in which silica prepared from commercial sodium silicate (CSS) at the same silica content on mechanical, morphological, and thermal properties.

2. Materials and Methods

2.1. Materials

Natural rubber latex (NRL) with 60wt% dry rubber content (DRC) and high ammonia (HA) treated with latex was purchased from Chemical & Material Co., Ltd. Carboxylated styrene-butadiene latex (XSBRL) was purchased from Jorakay Corporation Co., Ltd. Rice husk ash (RHA) from biomass power plant was purchased from Chia Meng Co., Ltd. Commercial sodium silicate (CSS) was purchased from Sigma-Aldrich Co., Ltd. Hydrochloric acid (HCl) was purchased from RCI Labscan Co., Ltd. Sodium hydroxide (NaOH) and acetic acid (CH_3COOH) were purchased from Carlo Erba Reagents. Stearic acid (SA), zinc oxide (ZnO), N-Cyclohexyl-2-Benzothiazole Sulfonamide (CBS), and sulfur (S) were supported by Chemical Innovation Co., Ltd.

2.2. Methods

2.2.1. Preparation of Sodium Silicate from RHA (RSS). RHA was purified by leaching RHA from biomass power plant with 1M HCl at 90°C by using magnetic stirrer for 3 h to remove some metallics. In the end of this process, the filter paper was used to filter unreacted RHA and DI water was used to wash unreacted RHA several times until the pH of unreacted RHA is neutral. And then, unreacted RHA was dried by using hot air oven at 110°C for 12 h and combusted by using muffle furnace at 600°C for 6 h to increase silica contents. RSS was prepared by dissolving the purified RHA that obtained from previous process with 1M NaOH at 90°C by using magnetic stirrer for 3 h and filter paper was used to filter unreacted RHA until obtain the clear solution that is RSS.

2.2.2. Preparation of NR/XSBR and NR/XSBR/Si Sheets. NR/XSBR/RSi sheets were prepared by mixing NRL to XSBRL at the ratio of 2:1, and RSS at various contents of silica (5, 10, and 15 phr) by using magnetic stirrer for 30 mins to obtain NR/XSBR/RSS mixtures. Acetic acid was dropped into NR/XSBR/RSS mixture until the pH of NR/XSBR/RSS mixture is neutral to precipitate silica. And then, the previous mixture was poured onto Teflon tray and dried at 60°C by using hot air oven for 72 h. For NR/XSBR/CSi sheet was prepared by using CSS at optimum silica content instead of RSS and following this process for comparing properties of NR/XSBR/Si composite at the same silica content

whereas silica was obtained from different sources. NR/XSBR sheet was also prepared by following this process whereas it was without sodium silicate mixing.

2.2.3. Preparation of NR/XSBR Blend and NR/XSBR/Si Composites. NR/XSBR and NR/XSBR/Si compounds were prepared by mixing NR/XSBR and NR/XSBR/Si sheets with 2 phr SA, 5 phr ZnO, 2.5 phr CBS, and 1 phr S by using two roll rubber mill. And then, the previous compound was vulcanized by using compression molding at 150°C with optimum curing time (t_c90) of each compound that was determined by Moving Die Rheometer (MDR, Gotech M2000) to obtain NR/XSBR blend and NR/XSBR/Si composites.

2.2.4. Chemical Properties. Energy Dispersive X-ray Fluorescence (EDXRF, Horiba XGT-5200) was used to characterize the chemical compositions of RHA, RSi, and CSi. RSi and CSi were prepared by dropping acetic acid into RSS and CSS was under magnetic stirrer until the pH of solution to neutral that grained silica precipitating. And then, the previous substance was dried at 110°C by using hot air oven for 24 h to obtain silica from RSS and CSS.

2.2.5. Mechanical Properties. The tensile properties of NR/XSBR blend and NR/XSBR/Si composites were measured according to ASTM D412 by using Universal Testing Machine (UTM, Instron 5565) with load cell of 5 kN and crosshead speed of 500 mm/min on the standard dumbbell specimen. At least five specimens were tested to obtain the average value for tensile strength, percentage elongation, modulus at 100% (M100), and 300% elongation (M300). The hardness of NR/XSBR blend and NR/XSBR/Si composites were measured according to ASTM D2240 by using hardness tester (Bareiss, HPE II) with test method that is Shore A. It makes five determinations of hardness at different positions on the specimen at least 6 mm in thickness to obtain the average hardness value.

2.2.6. Morphological Properties. The tensile fracture surface of NR/XSBR blend, NR/XSBR/Si composites, and silica particles that precipitated from RSS and CSS were coated with gold before examined by Field Emission Scanning Electron Microscope (FE-SEM, Carl Zeiss Auriga).

2.2.7. Thermal Properties. Thermogravimetric analyzer (TGA, Mettler Toledo TGA/DSC 1) was used to analyze the thermal decomposition of NR/XSBR blend and NR/XSBR/Si composites that placed in alumina pan and heated from room temperature up to 800°C under nitrogen with heating rate of 10°C/min.

3. Results and Discussion

3.1. Chemical Properties of Silica

The chemical compositions of RHA, RSi, and CSi are listed in Table 1. RHA from biomass power plant shows the lowest percentage SiO_2 composition is 82.97%. RSi shows percentage chemical compositions are similar to CSi and contain percentage SiO_2 composition approximately 97% indicating the RHA that can preparate silica similarity to commercial grade.

Table 1. Chemical compositions of RHA, RSi, and CSi.

	Al_2O_3	SiO_2	K_2O	CaO	TiO_2	MnO_2	Fe_2O_3
RHA	-	82.97	9.78	3.31	0.13	2.68	1.13
RSi	2.27	97.20	0.34	0.10	0.03	-	0.05
CSi	2.38	97.28	0.11	0.06	0.06	-	0.11

IUMRS-ICA 2021 IOP Publishing
Journal of Physics: Conference Series **2175** (2022) 012017 doi:10.1088/1742-6596/2175/1/012017

3.2. Morphological Properties of Silica

The morphological images of RSi and CSi are shown in Figure 1. RSi and CSi show silica particles with a size that is lower than 100 nm in a general form that is spherical structure and partially agglomerate owing to filler-filler interactions of silica (13, 14). On the other hand, RSi shows smaller particle size and lower agglomeration than CSi.

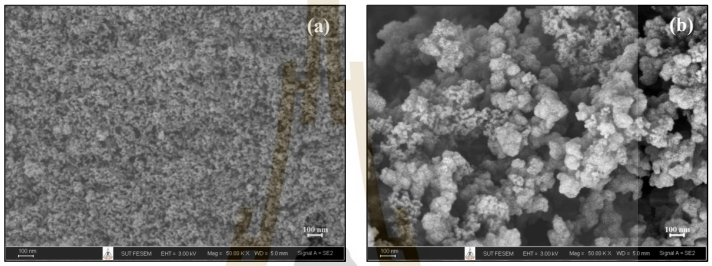

Figure 1. SEM images of (a) RSi and (b) CSi.

3.3. Mechanical Properties of NR/XSBR/Si Composites

The mechanical properties in terms of M100, M300, tensile strength, percentage elongation, and hardness of NR/XSBR blend and NR/XSBR/Si composites that blended with RSi at 5, 10, and 15 phr and CSi at 10 phr are shown in Figure 2. NR/XSBR blend shows the highest percentage elongation approximately 840% indicating the general rubber properties that is an elastic characteristic. The containing silica at 10 phr in NR/XSBR blend can improve the tensile strength whereas silica sources show insignificant effect on this property. Nevertheless, NR/XSBR/Si composites show the percentage elongation slightly decrease. The increasing silica contents in NR/XSBR blend show the mechanical properties in terms of M100, M300, and hardness are higher values than NR/XSBR blend because fillers with a higher stiffness than the matrix can increase the modulus of composite and value is higher when fillers increasing (15) whereas the silica sources also show insignificant effect on these properties.

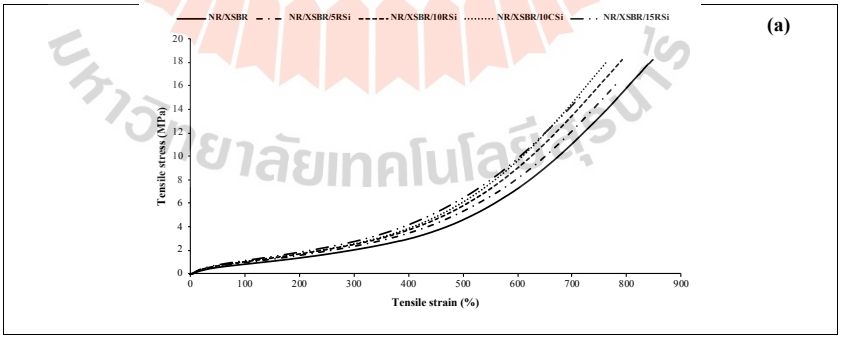

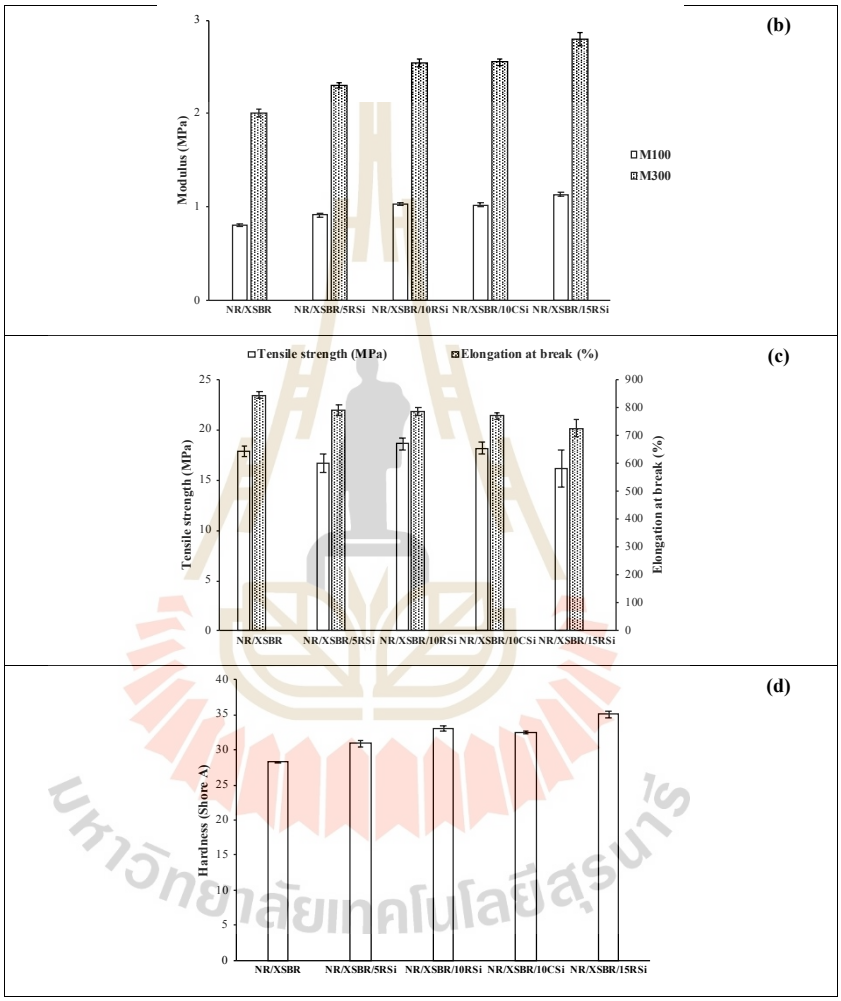

Figure 2. Mechanical properties of NR/XSBR blend and NR/XSBR/Si compositions showing (a) stress-strain curve, (b) modulus at 100% elongation and modulus at 300% elongation, (c) tensile strength and percentage elongation, and (d) hardness.

3.4. Morphological Properties of NR/XSBR/Si Composites

The morphological images of NR/XSBR blend and NR/XSBR/Si composites that blended with RSi at 5, 10, and 15 phr and CSi at 10 phr are shown in Figure 3. NR/XSBR blend shows holeless on tensile

IUMRS-ICA 2021 IOP Publishing
Journal of Physics: Conference Series **2175** (2022) 012017 doi:10.1088/1742-6596/2175/1/012017

fracture surface caused by filler detachment due to incompatibility between silica and rubber. In the same way, NR/XSBR/15RSi composite shows the highest holes number with a large-sized on tensile fracture surface owing to filler agglomeration that relates the lowest percentage elongation. The tensile fracture surfaces of NR/XSBR/10RSi and NR/XSBR/10CSi composites shows analogous images.

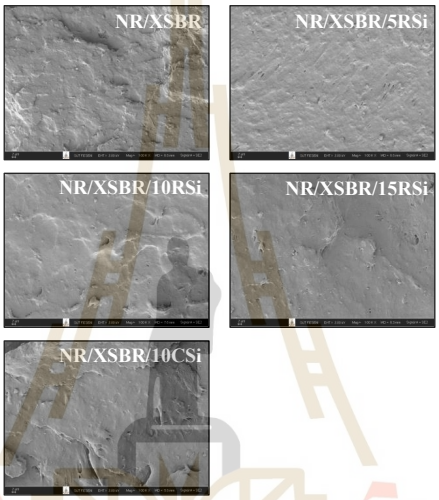

Figure 3. SEM images of NR/XSBR blend and NR/XSBR/Si composites.

3.5. Thermal Properties of NR/XSBR/Si Composites

The thermal properties in terms of degradation temperature at onset (T_{onset}), temperature at 50% weight loss level ($T_{50\%}$), temperature at maximum weight loss level (T_{max}), percentage residue, and percentage weight loss level at maximum degradation temperature (%wt. loss at T_{max}) of NR/XSBR blend and NR/XSBR/Si composites blended with RSi at 5 and 10 phr and CSi at 10 phr are listed in Table 2. The containing silica in NR/XSBR blend can improve the thermal stability of rubber as shown clearly in terms of $T_{50\%}$, T_{max}, and %wt. loss at T_{max}. $T_{50\%}$ and T_{max} of NR/XSBR/Si composites are higher temperatures than NR/XSBR blend whereas %wt. loss at T_{max} of NR/XSBR/Si composites lower than that of NR/XSBR blend. This may be due to the strong interaction of silanol group of silica with carboxylic group of XSBR. On the other hand, the contents and sources of silica play insignificant effect on the degradation temperature of NR/XSBR/Si composites.

Table 2. Thermal characteristics of NR/XSBR blend and NR/XSBR/Si composites.

Sample	T_{onset} (°C)	$T_{50\%}$ (°C)	T_{max} (°C)	%wt. loss at T_{max} (%)	Residue (%)
NR/XSBR	351	390	387	47.36	4.13
NR/XSBR/5RSi	352	400	392	43.75	9.40
NR/XSBR/10RSi	353	403	393	42.44	12.00
NR/XSBR/10CSi	352	400	391	43.49	14.67

4. Conclusions

Silica can be successfully prepared from RHA which comparable to commercial grade containing 97% SiO_2 composition and silica particle size is lower than 100 nm. The increasing silica contents in NR/XSBR blend improve modulus and hardness. NR/XSBR/10Si composites show the highest tensile strength. Silica sources show insignificant effect on mechanical properties. Higher decomposition temperature of NR/XSBR was obtained with the addition of silica.

Acknowledgments

The authors are grateful for financial support from the Center of Excellence on Petrochemical and Materials Technology (PETROMAT) and chemicals support that used in rubber compounding from the Chemical Innovation Co., Ltd.

References

[1] Chuayjuljit S, Nutchapong T, Saravari O, Boonmahitthisud A. Preparation and characterization of epoxidized natural rubber and epoxidized natural rubber/carboxylated styrene butadiene rubber blends. Journal of Metals, Materials and Minerals. 2015;25(1).

[2] Vu CM, Vu HT, Choi HJ. Fabrication of natural rubber/epoxidized natural rubber/nanosilica nanocomposites and their physical characteristics. Macromolecular Research. 2015;23(3):284-90.

[3] Rajan V, Dierkes WK, Joseph R, Noordermeer JW. Science and technology of rubber reclamation with special attention to NR-based waste latex products. Progress in polymer science. 2006;31(9):811-34.

[4] Jones K, Tinker A. Blends of natural rubber: Novel techniques for blending with specialty polymers: Springer Science & Business Media; 1997.

[5] Varkey JT, Augustine S, Thomas S. Thermal degradation of natural rubber/styrene butadiene rubber latex blends by thermogravimetric method. Polymer-Plastics Technology and Engineering. 2000;39(3):415-35.

[6] Motaung TE, Luyt AS, Thomas S. Morphology and properties of NR/EPDM rubber blends filled with small amounts of titania nanoparticles. Polymer Composites. 2011;32(8):1289-96.

[7] Le HH, Ilisch S, Heidenreich D, Wutzler A, Radusch HJ. Kinetics of the phase selective localization of silica in rubber blends. Polymer composites. 2010;31(10):1701-11.

[8] Shan C, Gu Z, Wang L, Li P, Song G, Gao Z, et al. Preparation, characterization, and application of NR/SBR/Organoclay nanocomposites in the tire industry. Journal of Applied Polymer Science. 2011;119(2):1185-94.

[9] Stephen R, Thomas S, Joseph K. Gas permeation studies of natural rubber and carboxylated styrene–butadiene rubber latex membranes. Journal of applied polymer science. 2005;98(3):1125-34.

[10] Poompradub S, Thirakulrati M, Prasassarakich P. In situ generated silica in natural rubber latex via the sol–gel technique and properties of the silica rubber composites. Materials Chemistry and Physics. 2014;144(1-2):122-31.

[11] Moayedi H, Aghel B, Nguyen H, Rashid ASA. Applications of rice husk ash as green and sustainable biomass. Journal of Cleaner Production. 2019;237:117851.

[12] Vaikuntam SR, Bhagavatheswaran ES, Xiang F, Wießner S, Heinrich G, Das A, et al. Friction, abrasion and crack growth behavior of in-situ and ex-situ silica filled rubber composites. Materials. 2020;13(2):270.

[13] Choi SS. Improvement of properties of silica-filled styrene–butadiene rubber compounds using acrylonitrile–butadiene rubber. Journal of applied polymer science. 2001;79(6):1127-33.

[14] Stephen R, Siddique A, Singh F, Kailas L, Jose S, Joseph K, et al. Thermal degradation and ageing behavior of microcomposites of natural rubber, carboxylated styrene butadiene rubber latices, and their blends. Journal of applied polymer science. 2007;105(2):341-51.

[15] Boonmahitthisud A, Chuayjuljit S. NR/XSBR nanocomposites with carbon black and carbon nanotube prepared by latex compounding. Journal of Metals, Materials and Minerals. 2012;22(1).

BIOGRAPHY

Miss Namthip Bureewong was born on March 2, 1996, in Rayong, Thailand. In 2017, she graduated with a bachelor's degree in polymer engineering from Suranaree University of Technology, in Nakhon Ratchasima, Thailand. Her bachelor's degree was entitled "Preparation of calcium carbonate from mussel shell for using as a filler in natural rubber and epoxidized natural rubber". In 2018, she started her master's degree study in materials engineering (polymer), Institute of Engineering, Suranaree University of Technology. Her master's degree was entitled "Development of natural rubber composite for cementitious materials", which was under the supervision of Assoc. Prof. Dr. Chaiwat Ruksakulpiwat and Assoc. Prof. Dr. Yupaporn Ruksakulpiwat. Her master's degree was supported by the Center of Excellence on Petrochemical and Materials Technology and the Research Center for Biocomposite Materials for Medical Industry and Agricultural and Food Industry. During the period of her study, several parts of her work were presented at the 5th International Conference on Smart Materials and Nanotechnology (SmartMat@2020) and published in the Suranaree Journal of Science and Technology. The 21st International Union of Materials Research Societies-International Conference in Asia (IUMRS-ICA 2020) and published in the Journal of Physics: Conference Series. The 37th International Conference of the Polymer Processing Society (PPS-37) and revised in the AIP Conference Proceedings.